Supporting information

Phosphonium carbosilane dendrimers for biomedical applications – synthesis, characterization and cytotoxicity evaluation

Authors:

Tomáš Strašák[1#], Jan Malý[2*], Dominika Wróbel[2], Marek Malý[2], Regina Herma[2], Jan Čermák[1], Monika Müllerová[1], Lucie Červenková Šťastná[1], Petra Cuřínová[1]

Affiliations:

[1]Institute of Chemical Process Fundamentals of the CAS, v.v.i, Prague, Czech Republic

[2]Department of Biology, J.E. Purkyně University, 40096 Usti nad Labem, Czech Republic

Corresponding authors address:

[#]Institute of Chemical Process Fundamentals of the CAS, v. v. i.

Rozvojova 2/135

CZ-165 02 Prague 6 - Suchdol

Czech Republic

strasak@icpf.cas.cz

*__University of J.E.Purkyně in Ústí nad Labem__

Department of Biology

České mládeže 8

40096 Ústí nad Labem

Czech Republic

malyjalga@seznam.cz

List of content

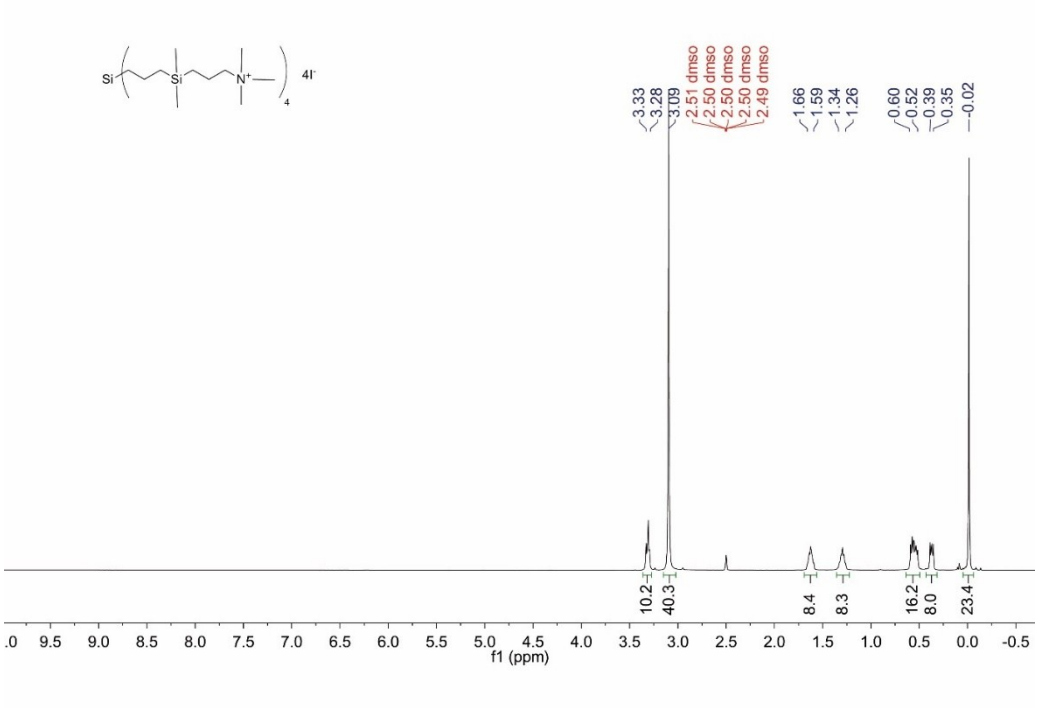

Figure SI1. ^{1}H NMR (500 MHz, DMSO-*d6*) of **7**.

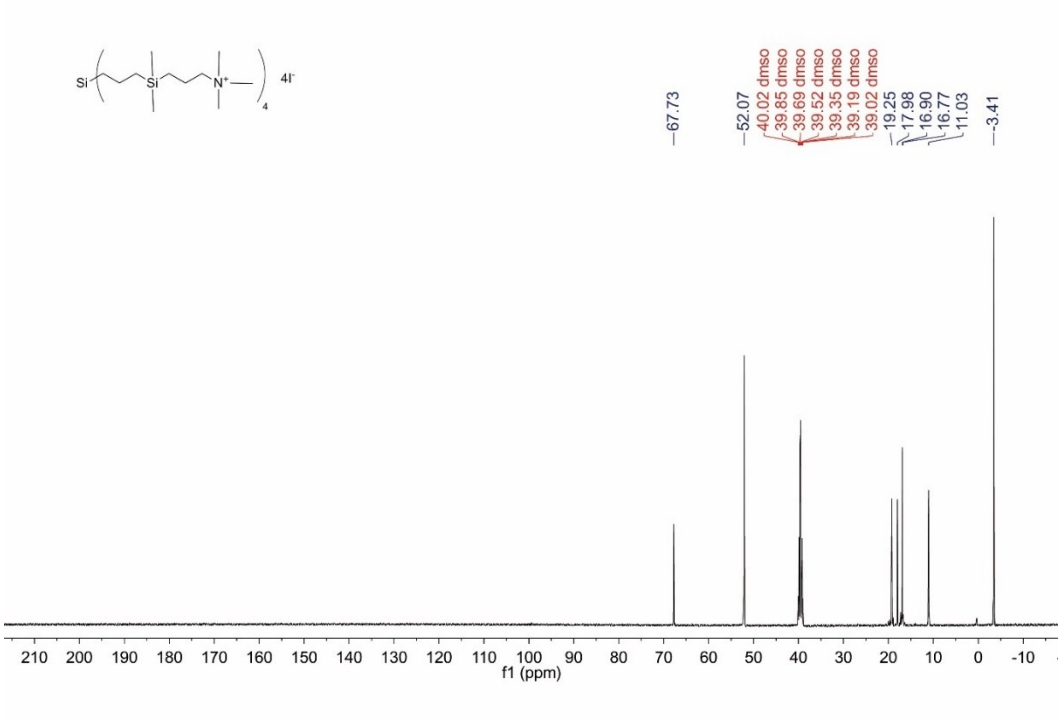

Figure SI2. ^{13}C {H} NMR (125 MHz, DMSO-*d6*) of **7**.

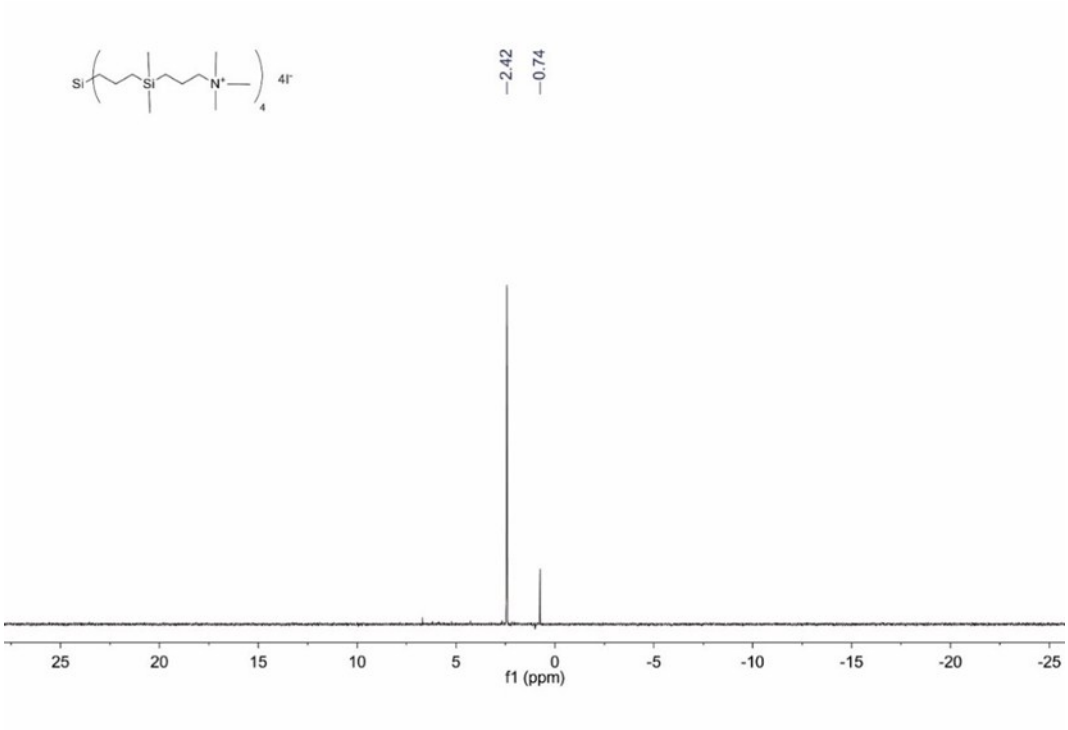

Figure SI3. ^{29}Si {H} NMR (99 MHz, DMSO-*d6*) of **7**.

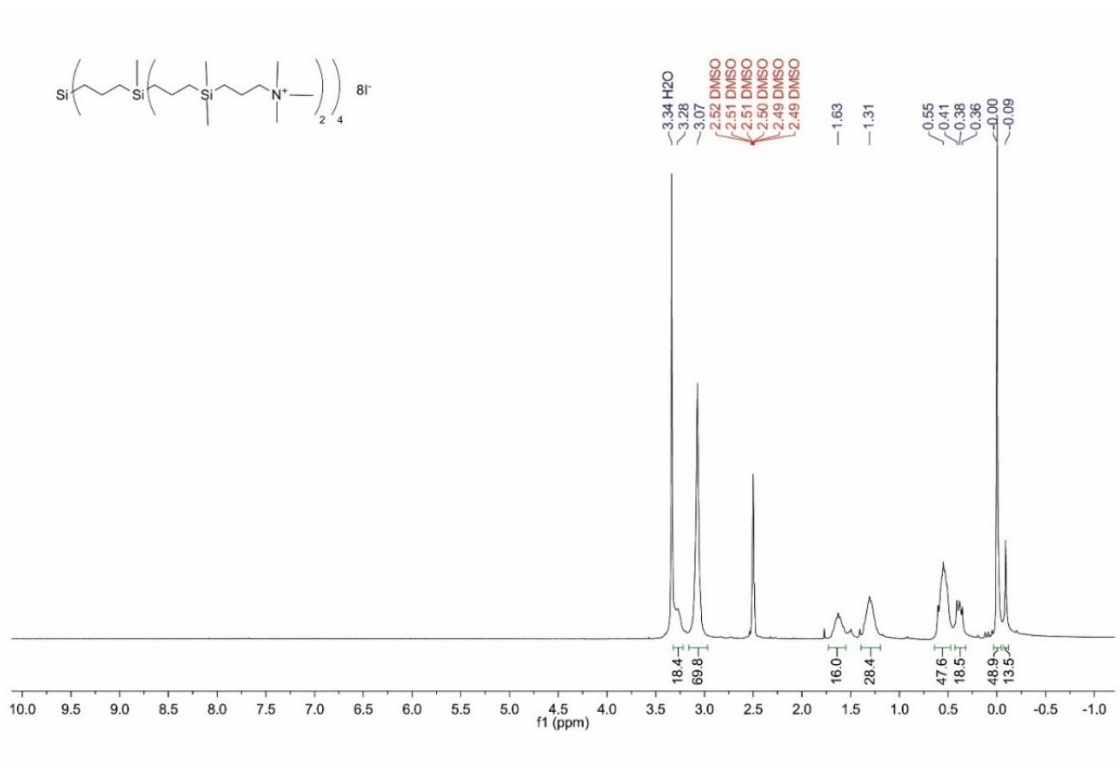

Figure SI4. ^{1}H NMR (300 MHz, DMSO-*d6*) of **8**.

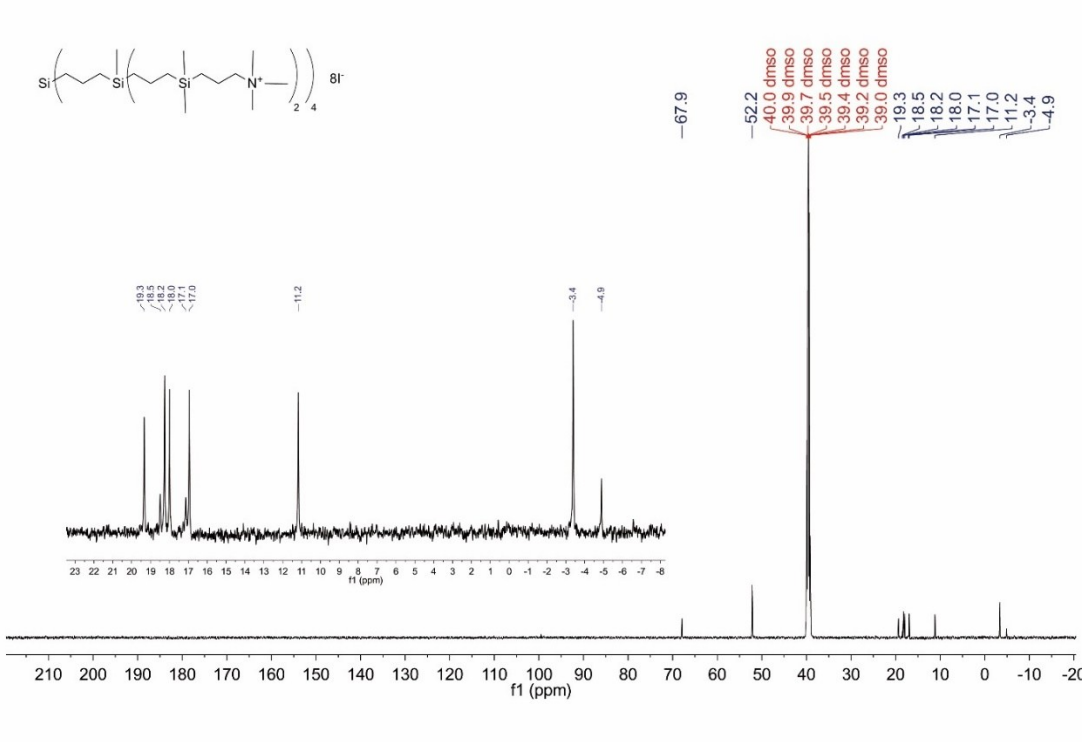

Figure SI5. ^{13}C {H} NMR (125 MHz, DMSO-*d6*) of **8**.

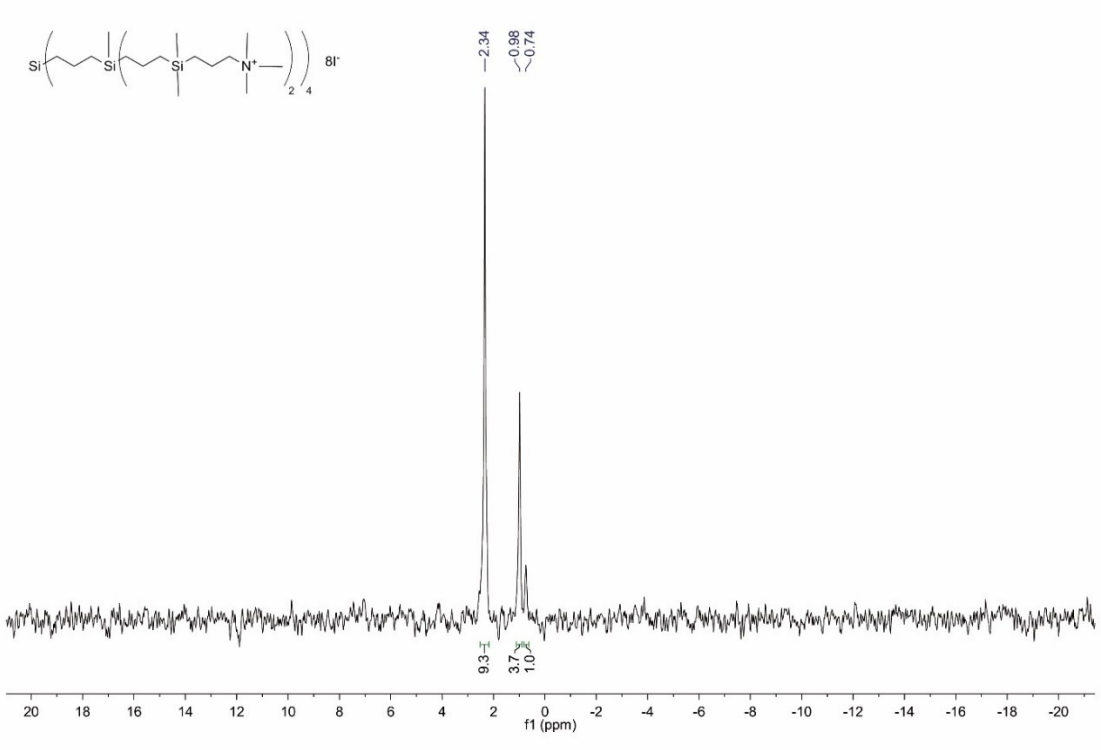

Figure SI6. ^{29}Si {H} NMR (59 MHz, DMSO-*d6*) of **8**.

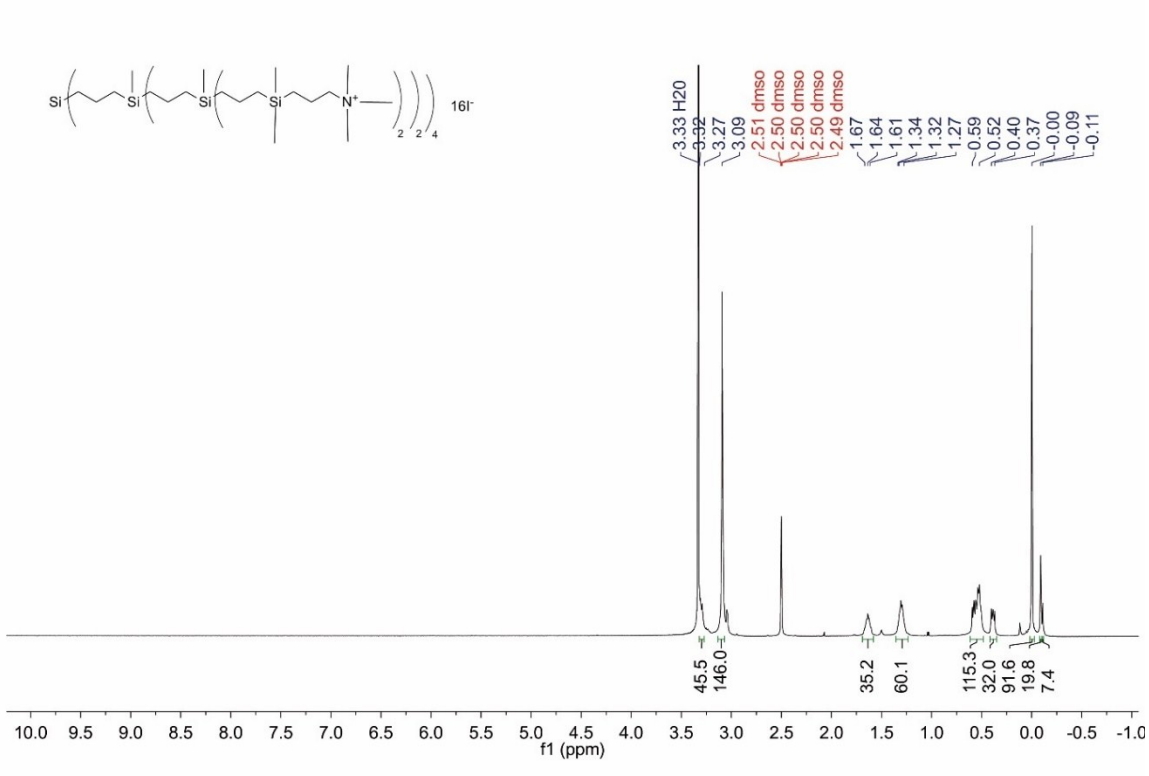

Figure SI7. 1H NMR (500 MHz, DMSO-d6) of 9.

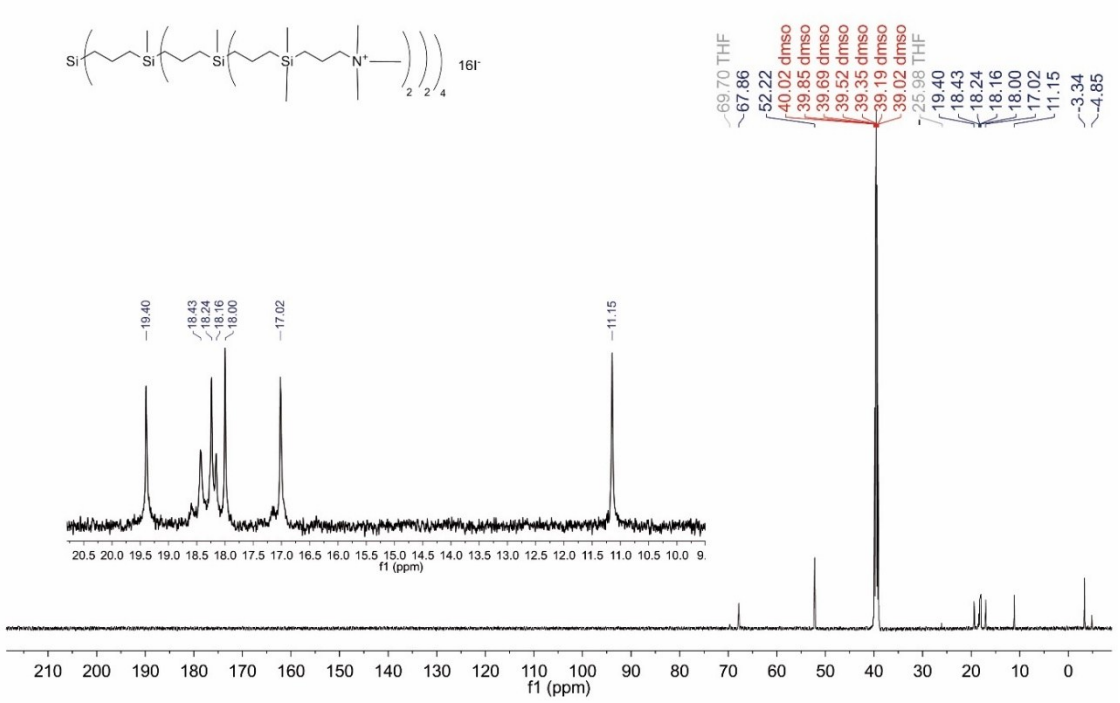

Figure SI8. ^{13}C {H} NMR (125 MHz, DMSO-*d6*) of **9**

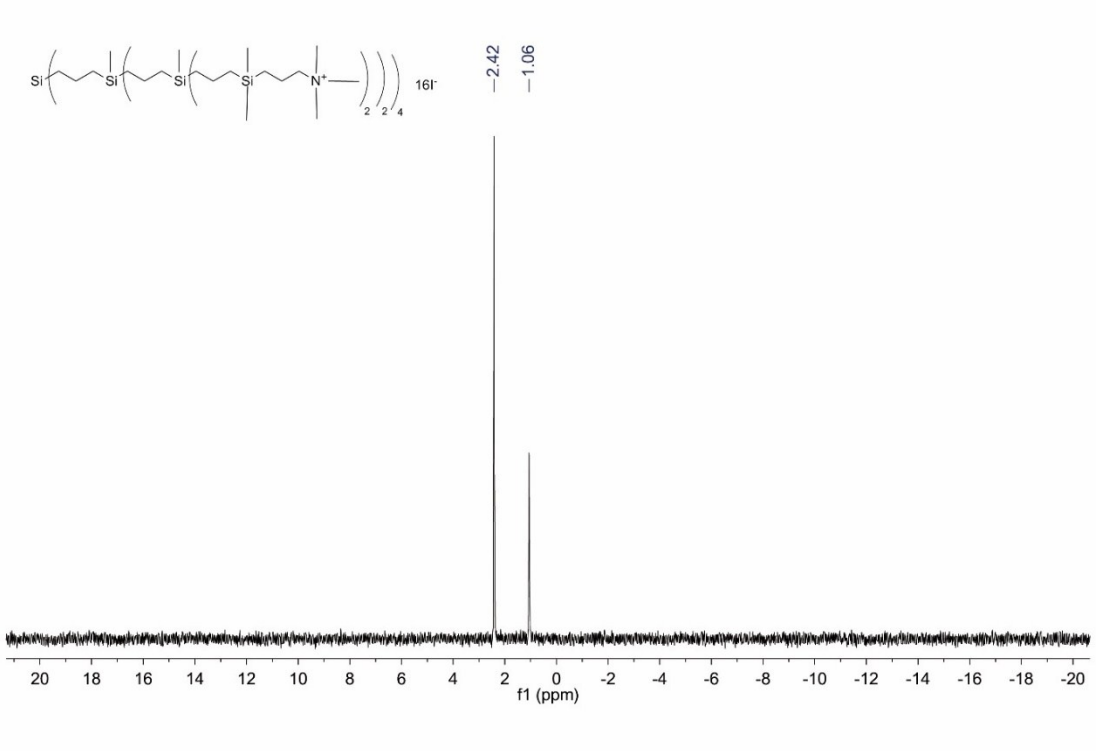

Figure SI9. ^{29}Si {H} Inept NMR (99 MHz, DMSO-*d6*) of **9**.

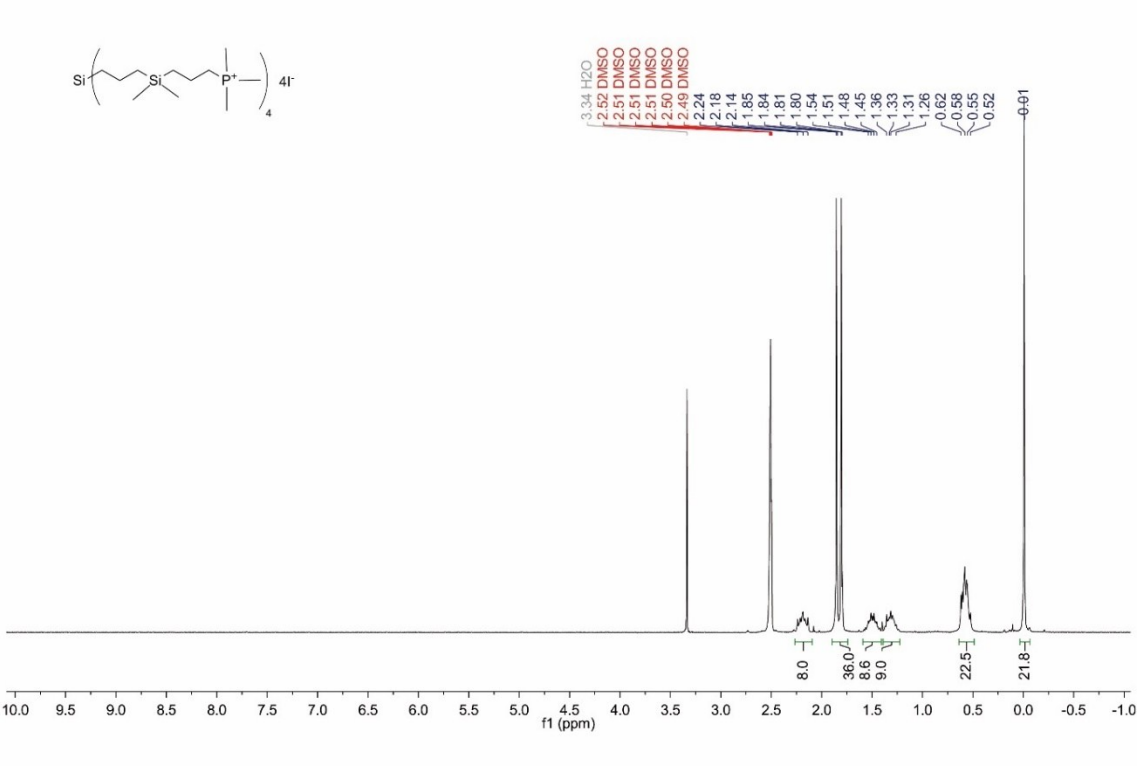

Figure SI10. ^{1}H NMR (300 MHz, DMSO-*d6*) of **10**.

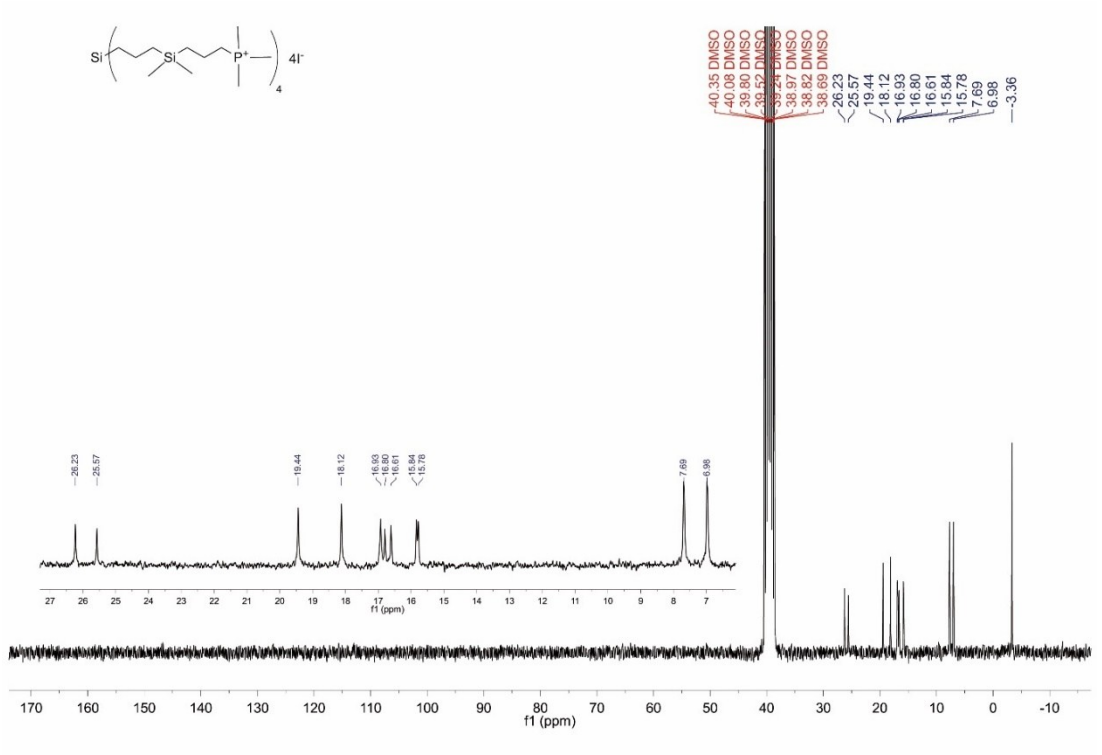

Figure SI11. ^{13}C {H} NMR (75 MHz, DMSO-*d6*) of **10**.

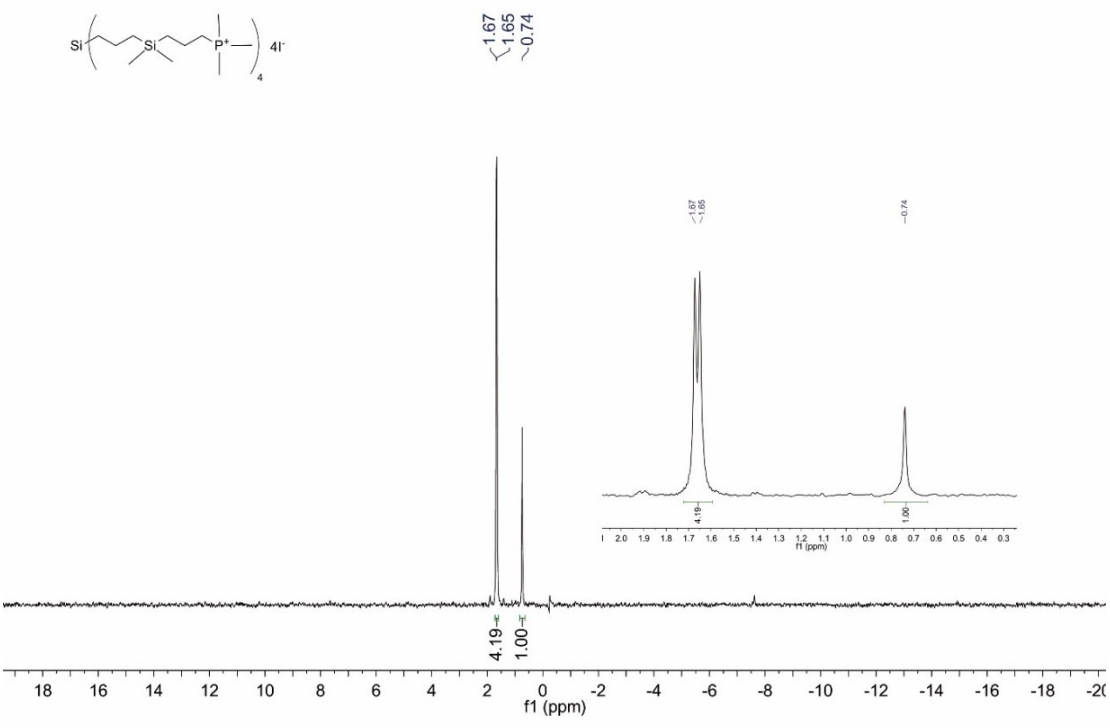

Figure SI12. ^{29}Si {H} NMR (59 MHz, DMSO-*d6*) of **10**.

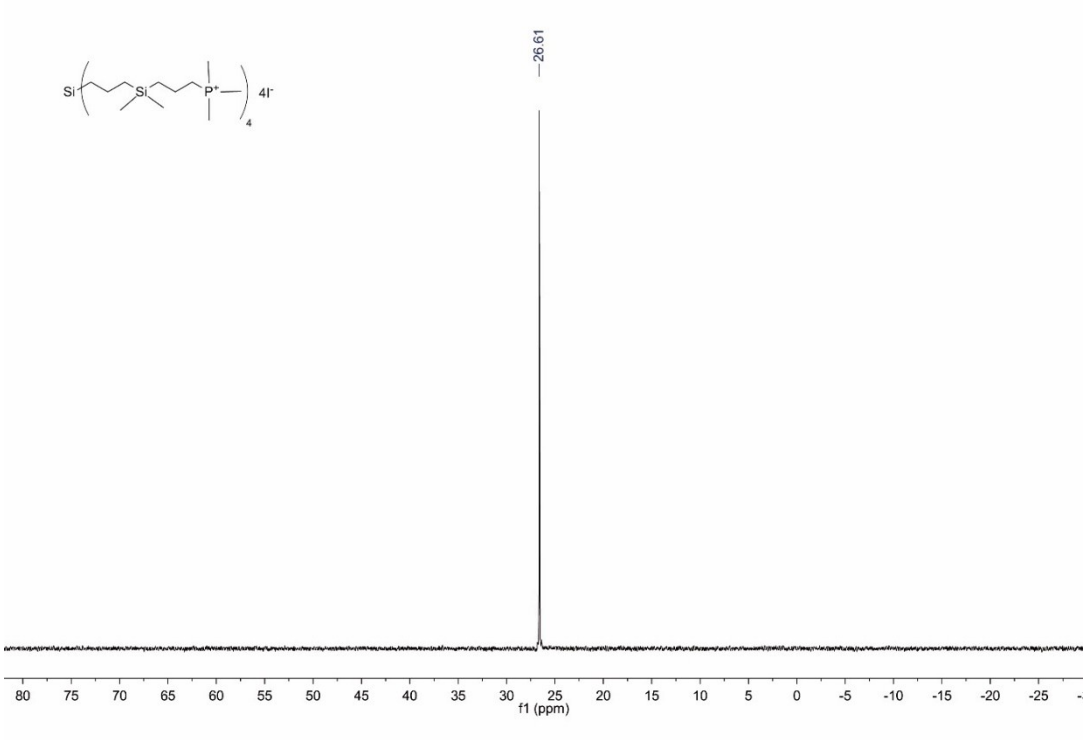

Figure SI13. $^{31}P\{H\}$ NMR (121 MHz, DMSO-*d6*) of **10**.

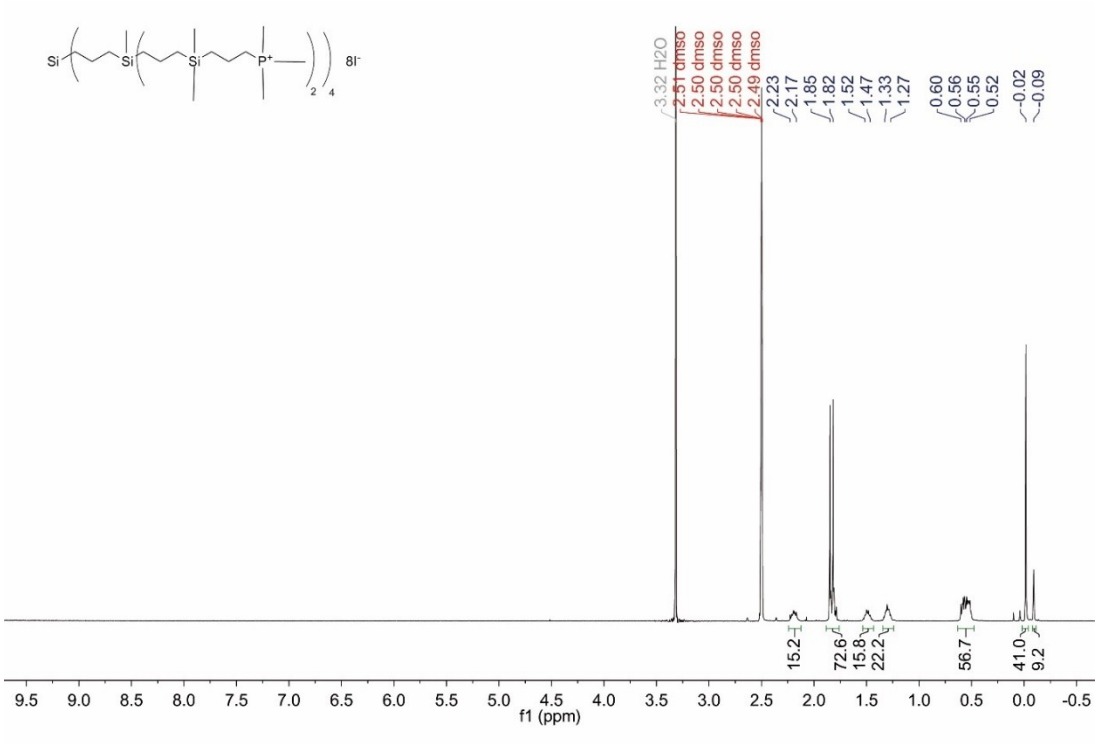

Figure SI14. ^{1}H NMR (500 MHz, DMSO-*d6*) of **11**.

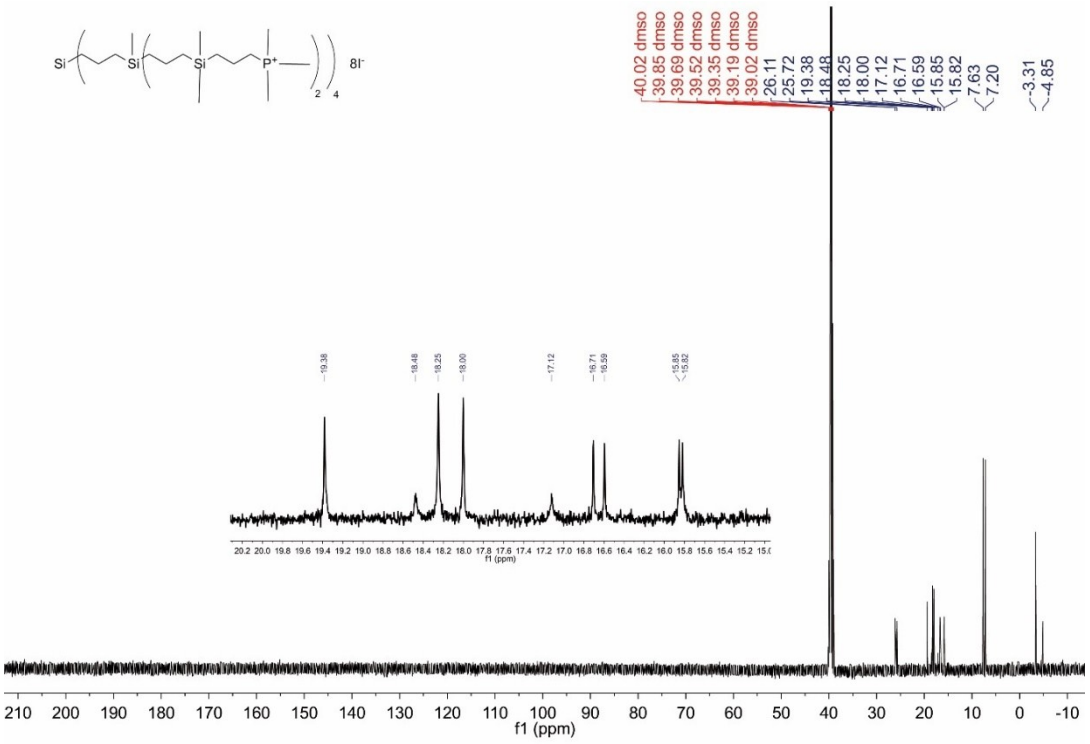

Figure SI15. ^{13}C {H} NMR (125 MHz, DMSO-*d6*) of **11**.

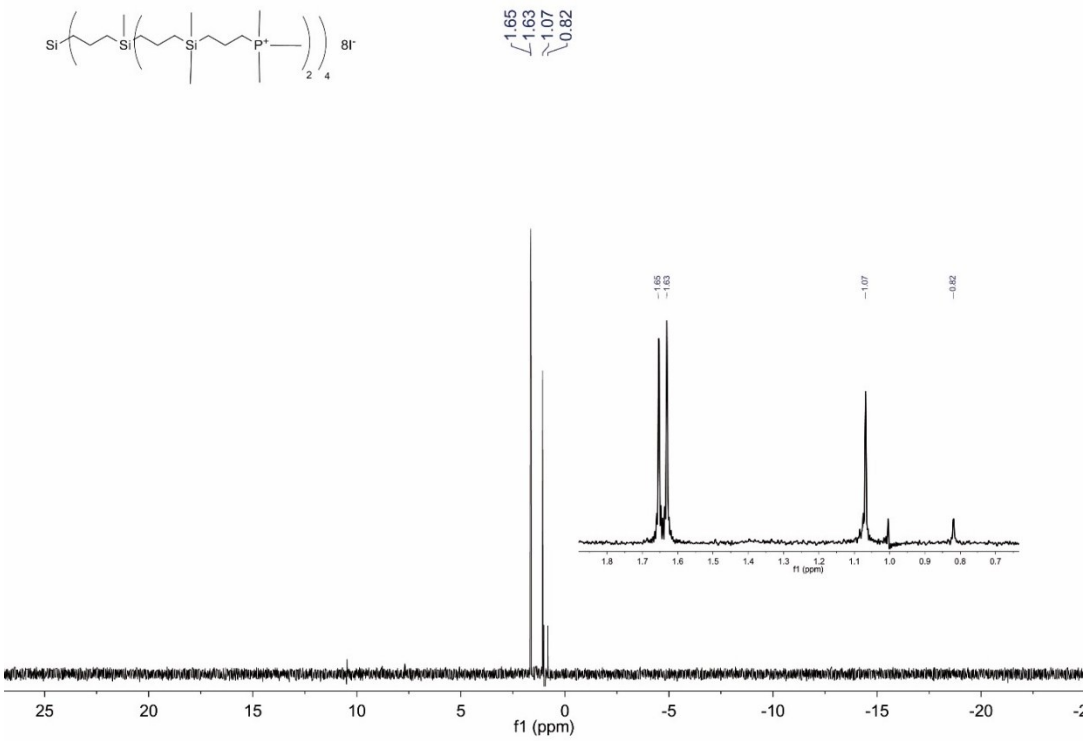

Figure SI16. ^{29}Si Inept {H} NMR (99 MHz, DMSO-*d6*) of **11**.

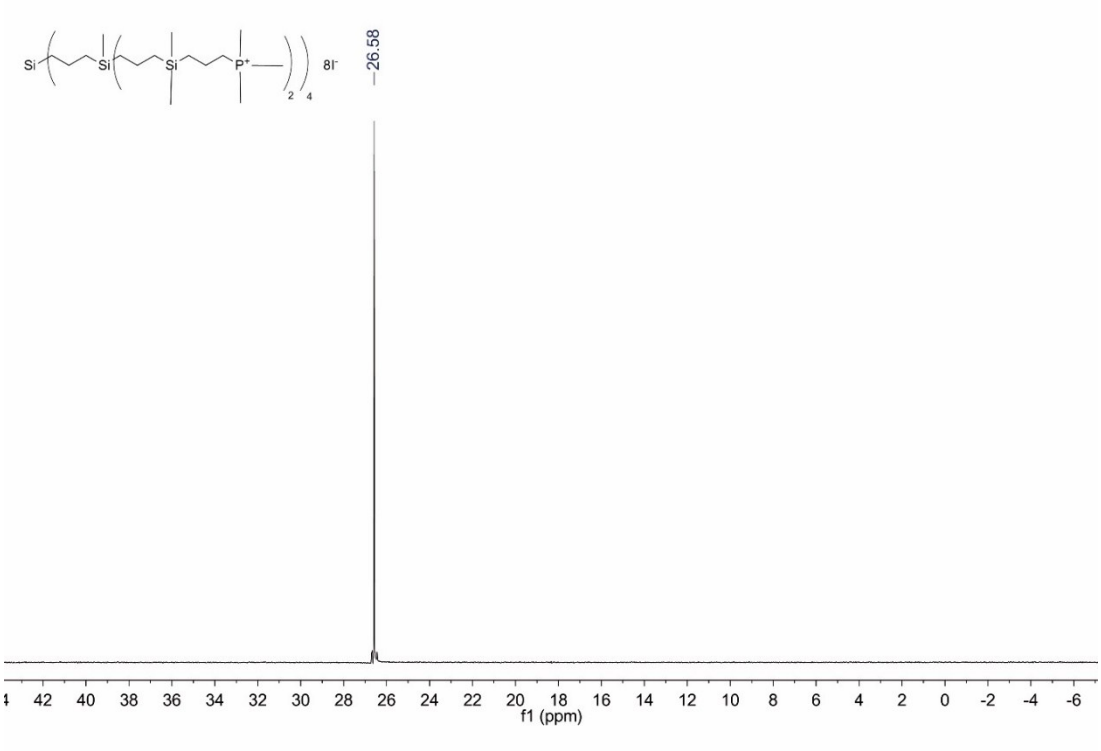

Figure SI17. $^{31}P\{H\}$ NMR (202 MHz, DMSO-*d6*) of **11**.

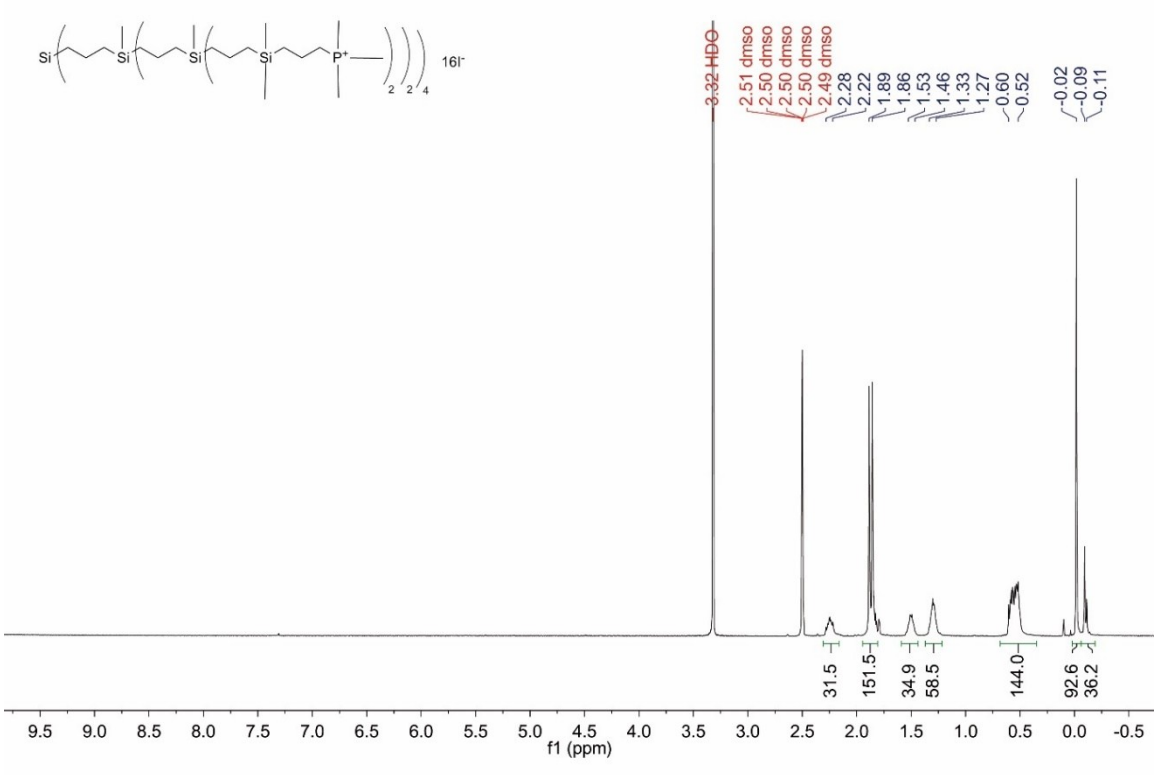

Figure SI18. ^{1}H NMR (500 MHz, DMSO-*d6*) of **12**.

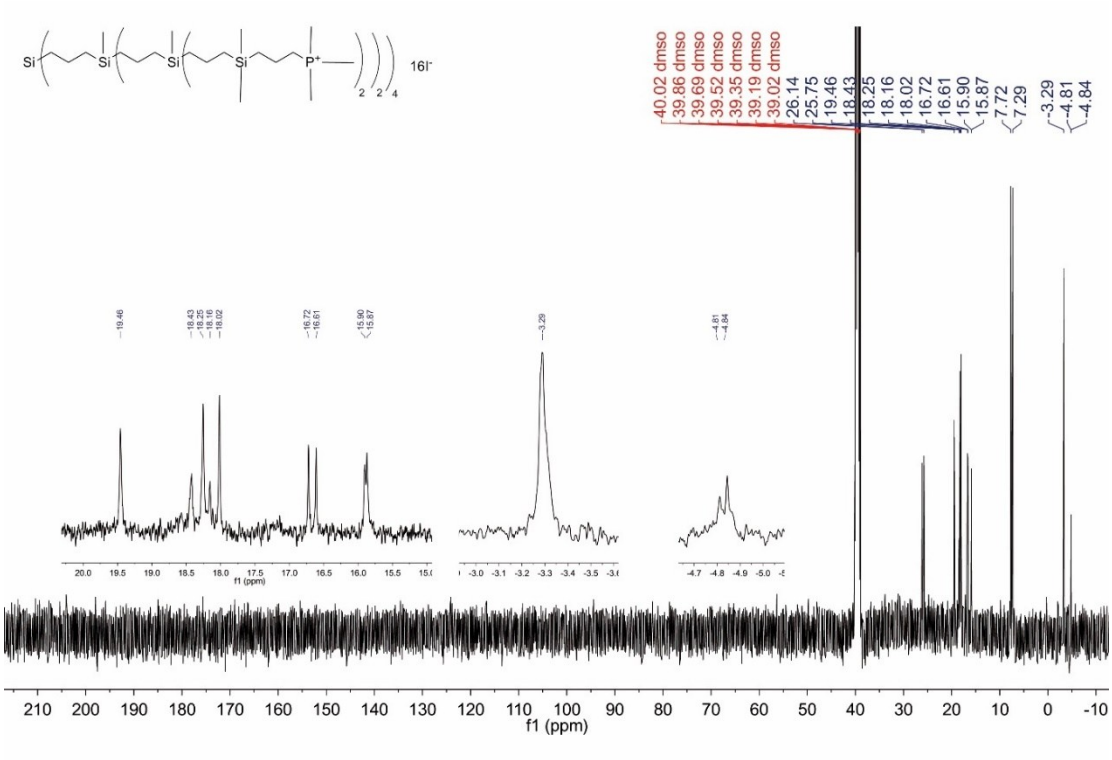

Figure SI19. ^{13}C {H} NMR (125 MHz, DMSO-*d6*) of **12**.

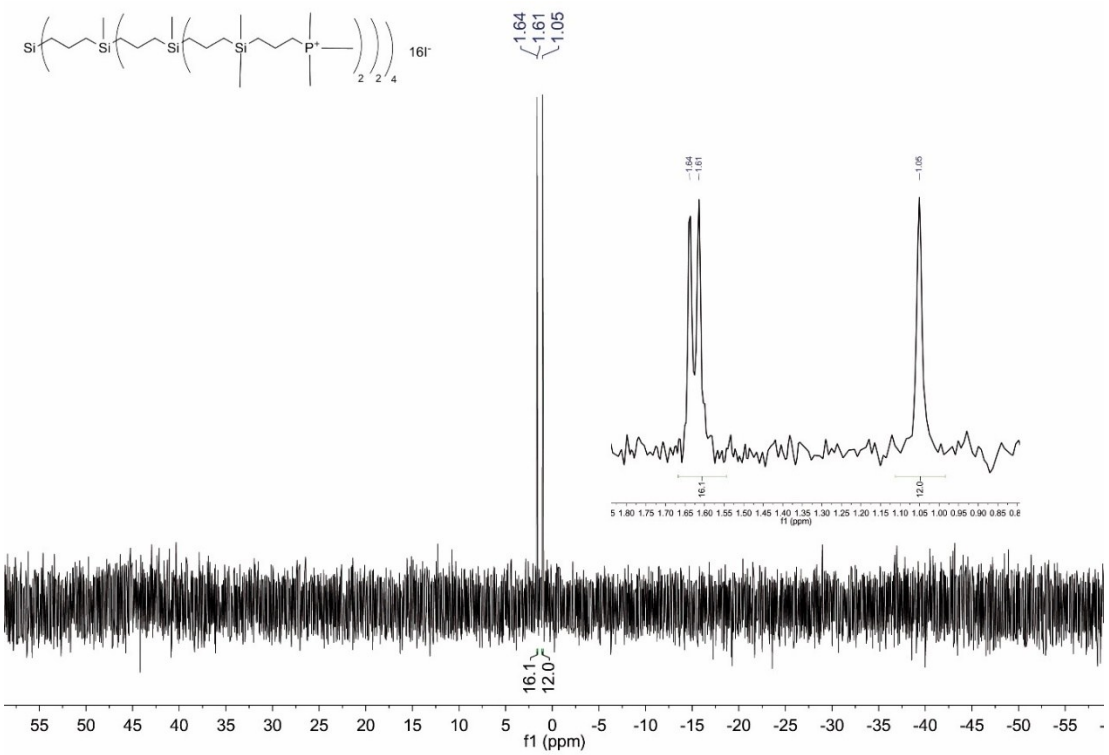

Figure SI20. ^{29}Si {H} NMR (99 MHz, DMSO-*d6*) of **12**.

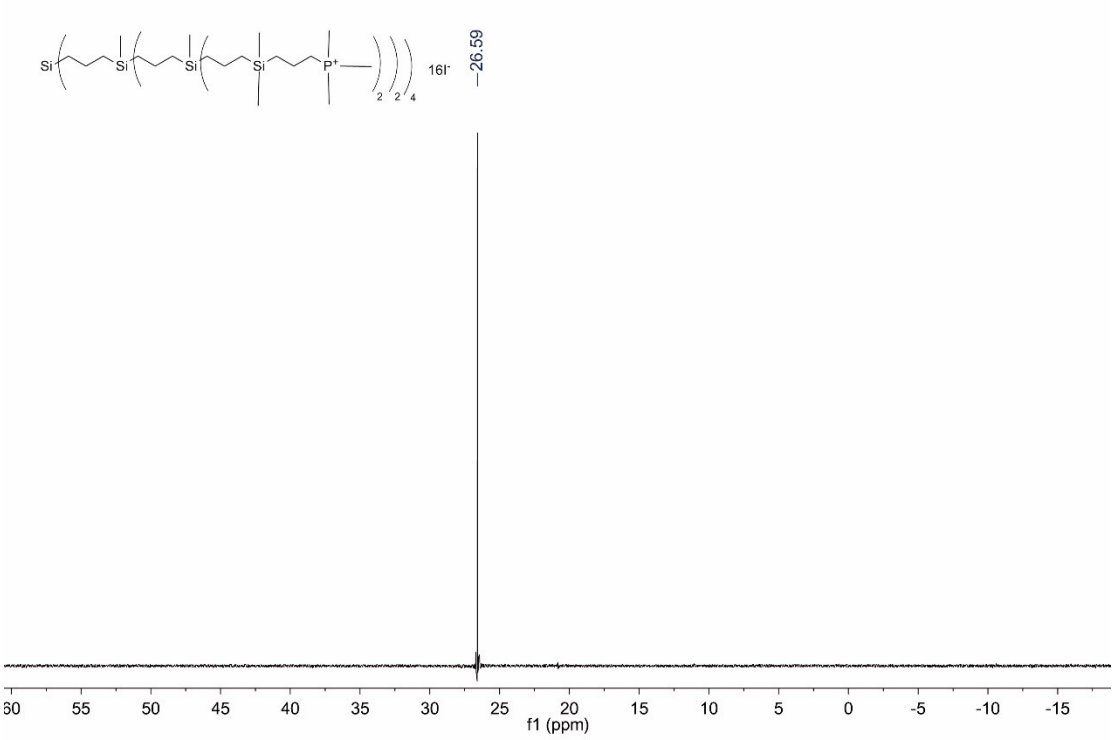

Figure SI21. $^{31}P\{H\}$ NMR (202 MHz, DMSO-*d6*) of **12**.

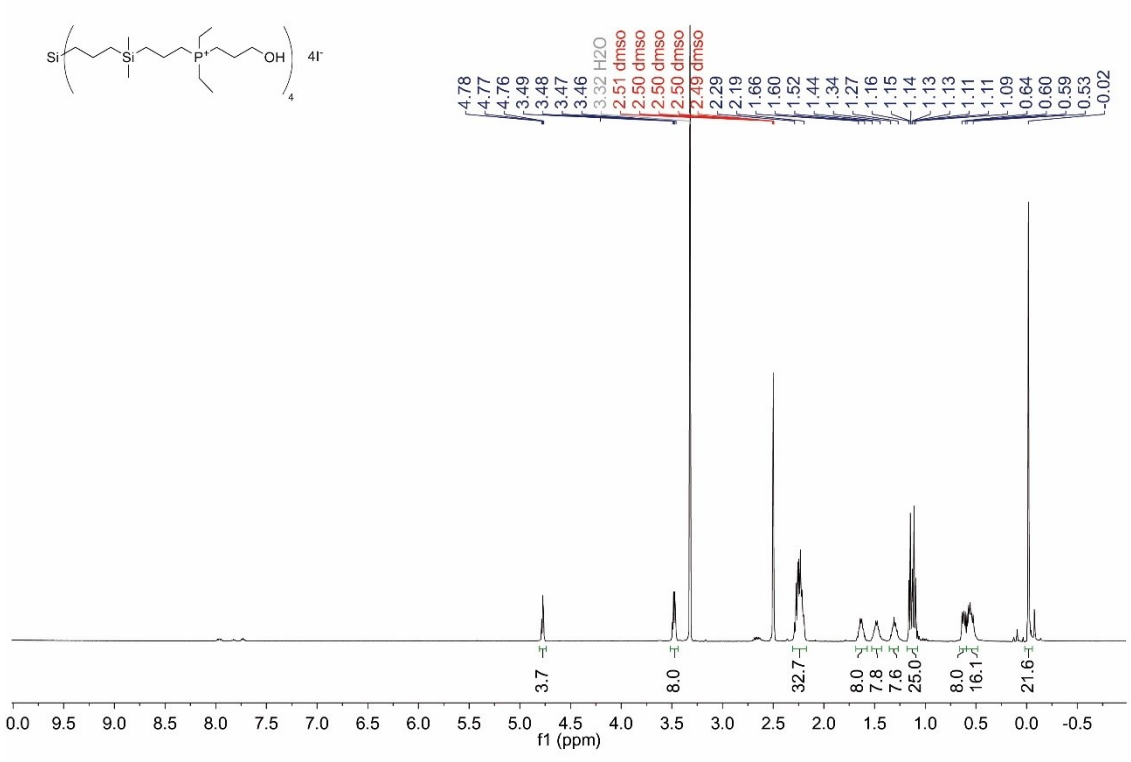

Figure SI22. ^{1}H NMR (500 MHz, DMSO-*d6*) of **13**.

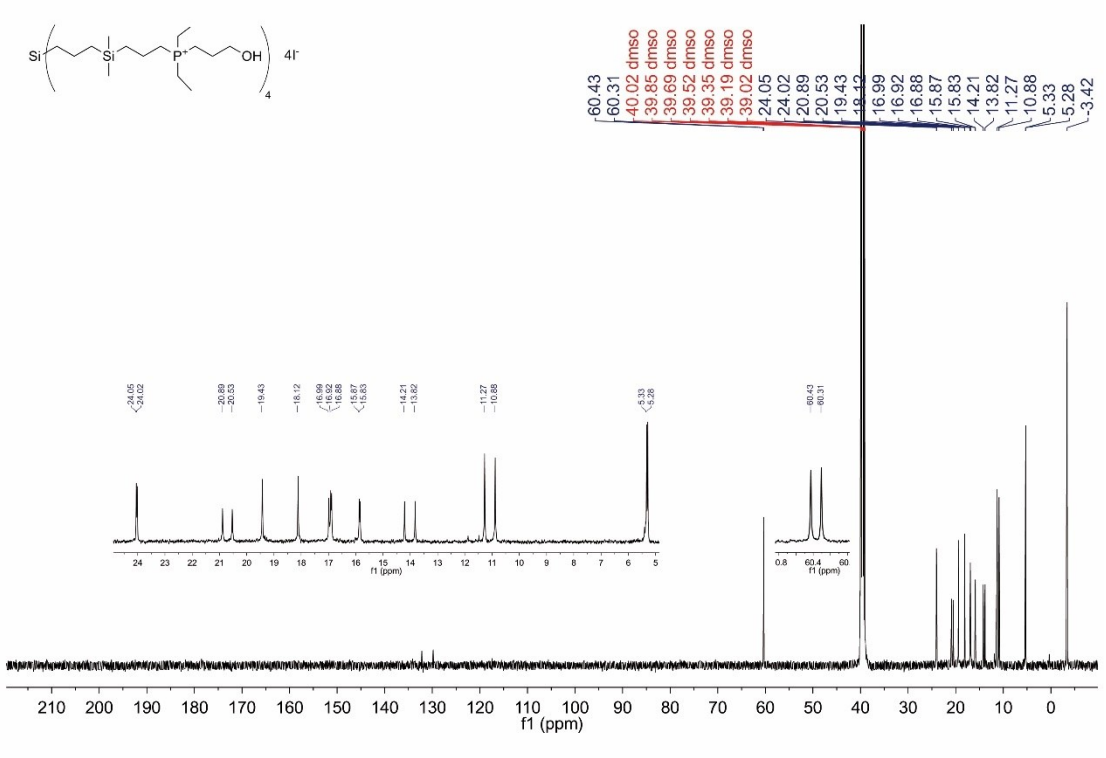

Figure SI23. ^{13}C {H} NMR (125 MHz, DMSO-*d6*) of **13**.

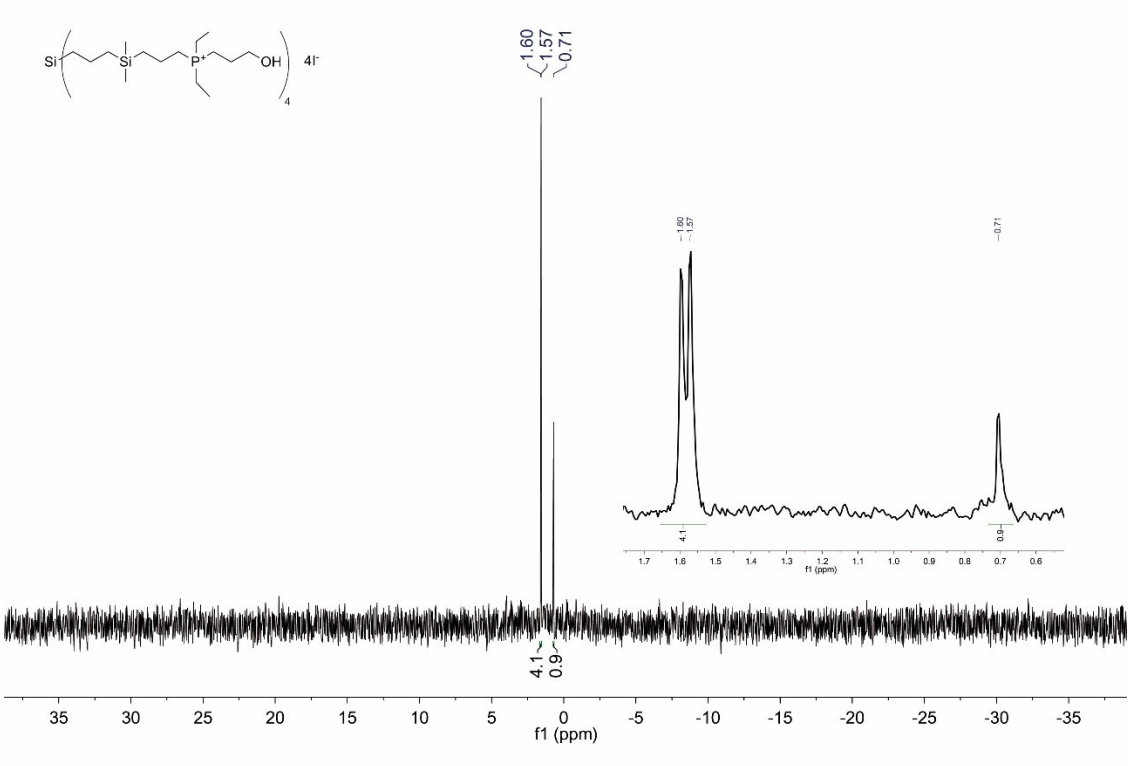

Figure SI24. ^{29}Si {H} NMR (99 MHz, DMSO-*d6*) of **13**.

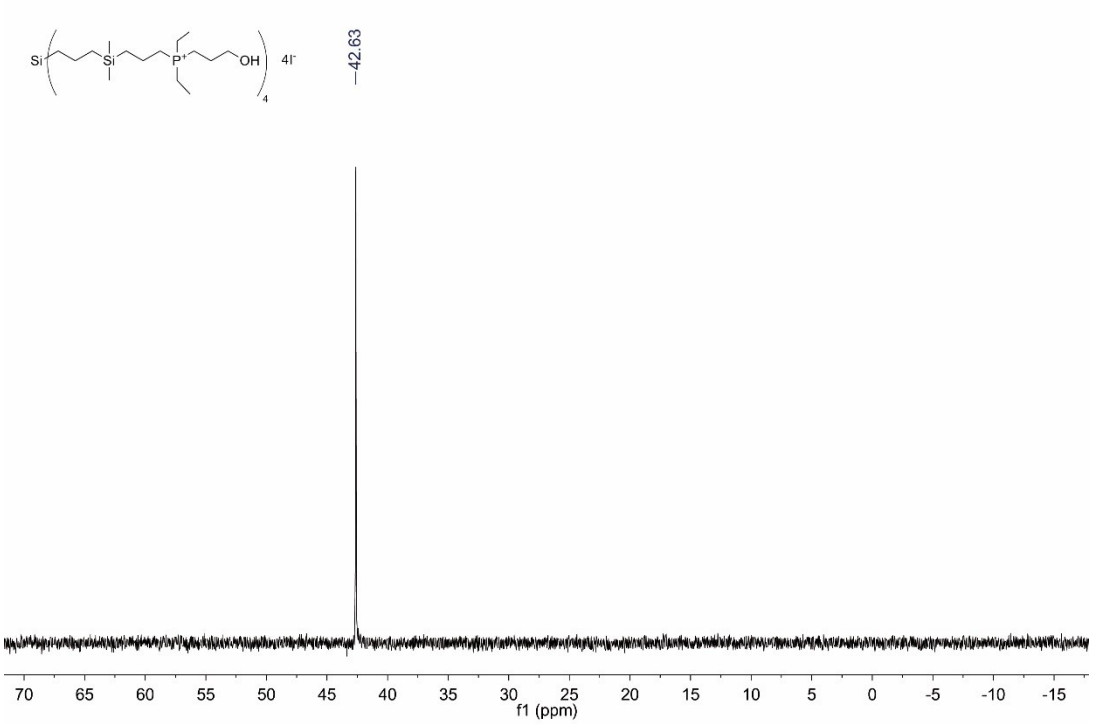

Figure SI25. $^{31}P\{H\}$ NMR (121 MHz, DMSO-*d6*) of **13**.

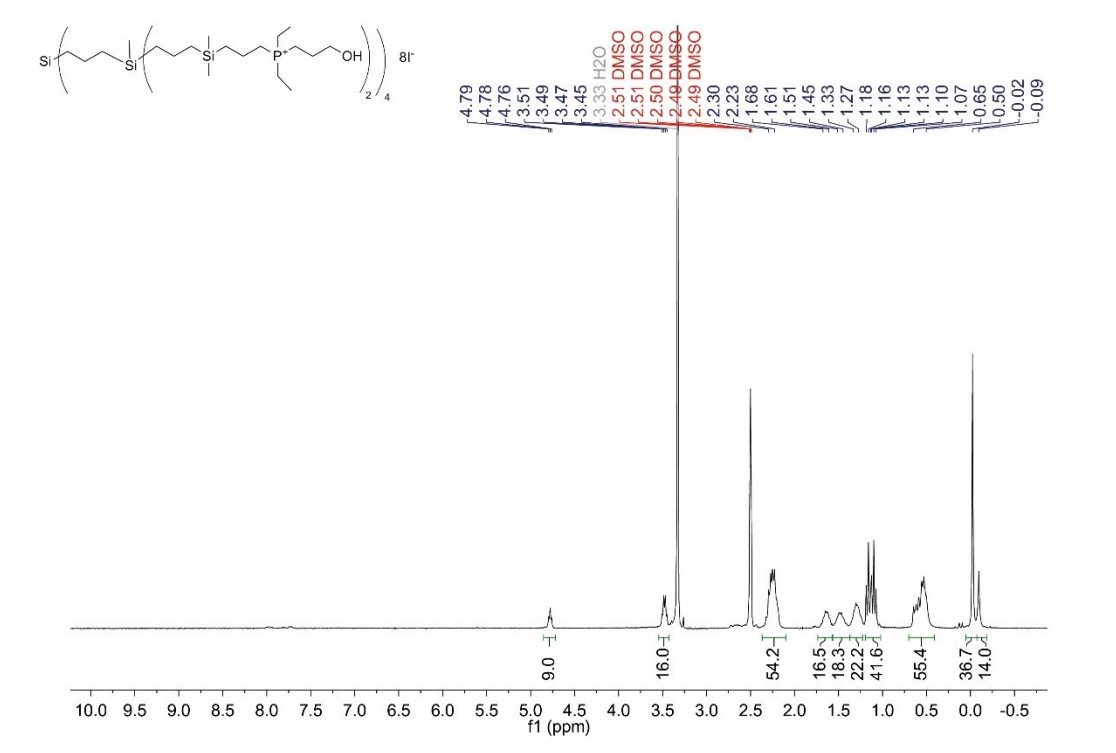

Figure SI26. ^{1}H NMR (300 MHz, DMSO-*d6*) of **14**.

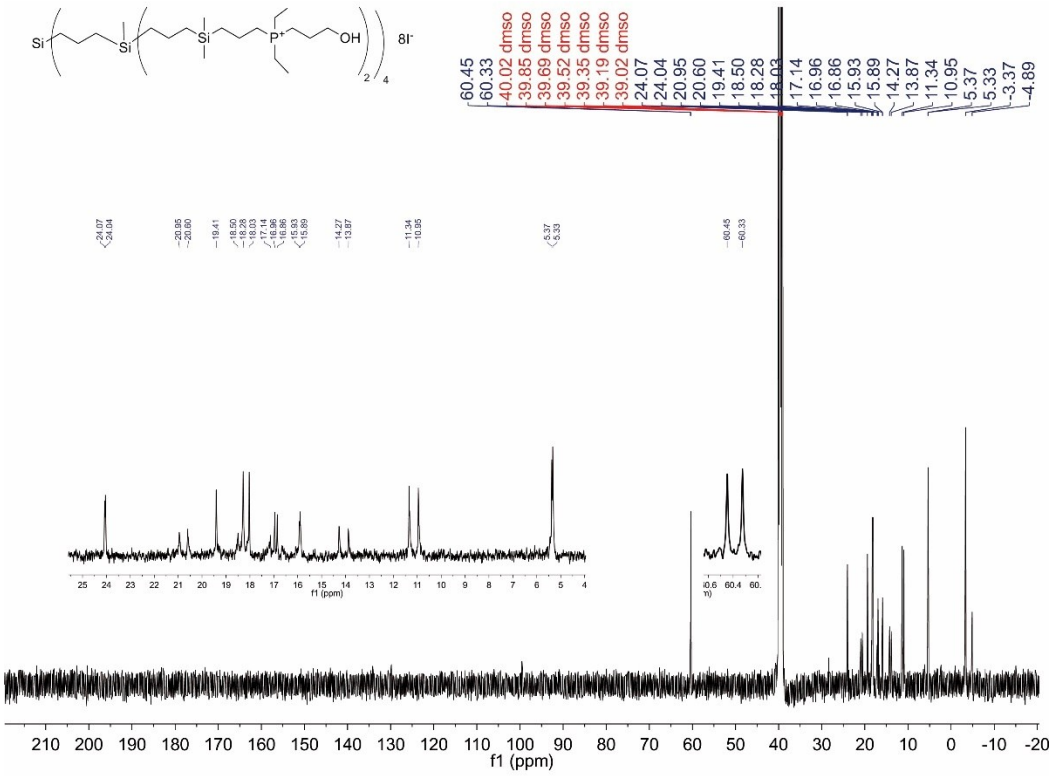

Figure SI27. ^{13}C {H} NMR (125 MHz, DMSO-*d6*) of **14**.

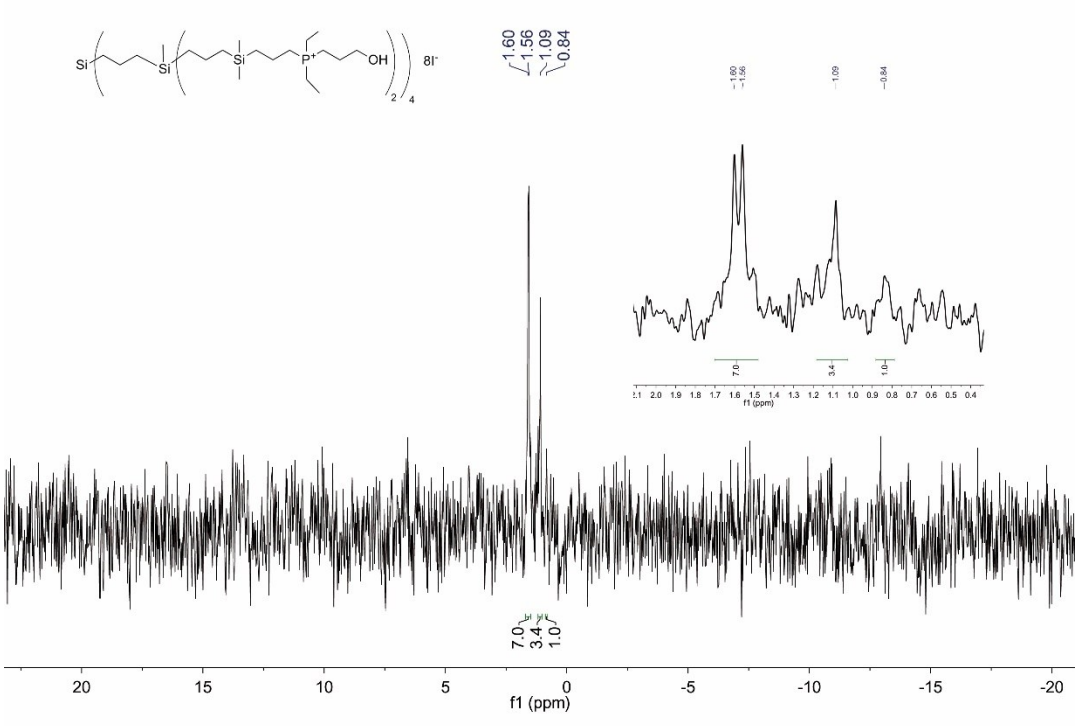

Figure SI28. ^{29}Si {H} NMR (59 MHz, DMSO-*d6*) of **14**.

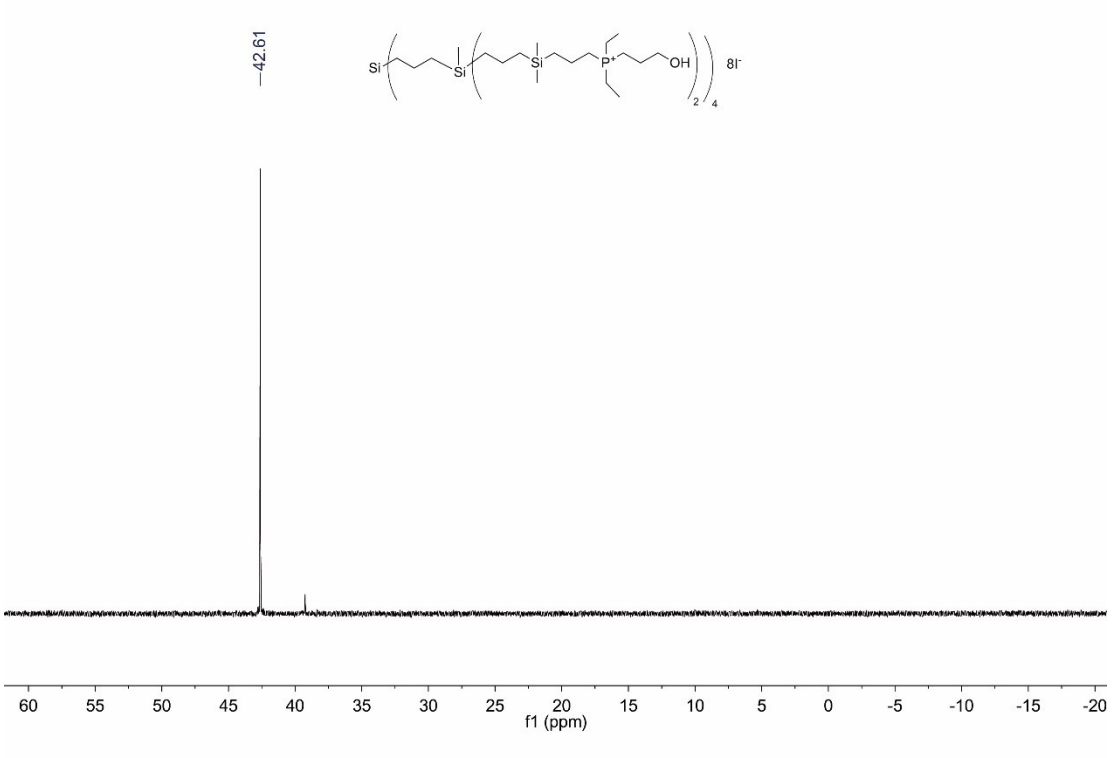

Figure SI29. $^{31}P\{H\}$ NMR (121 MHz, DMSO-*d6*) of **14**.

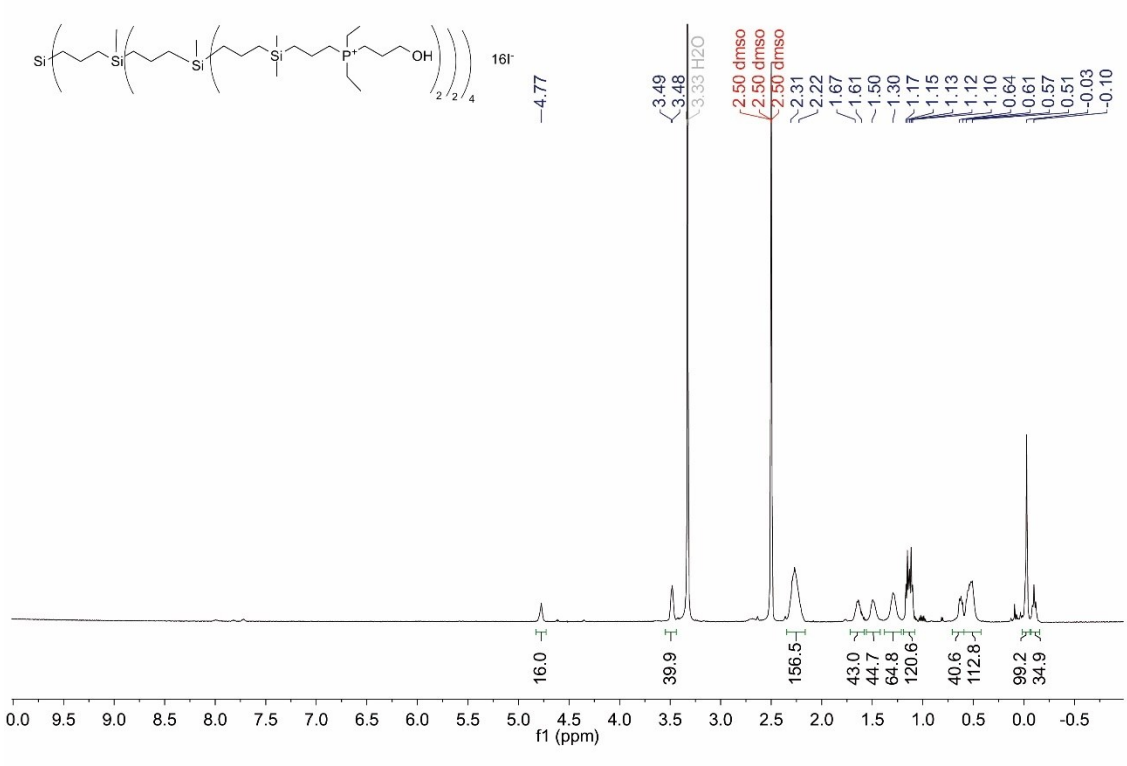

Figure SI30. ^{1}H NMR (500 MHz, DMSO-*d6*) of **15**.

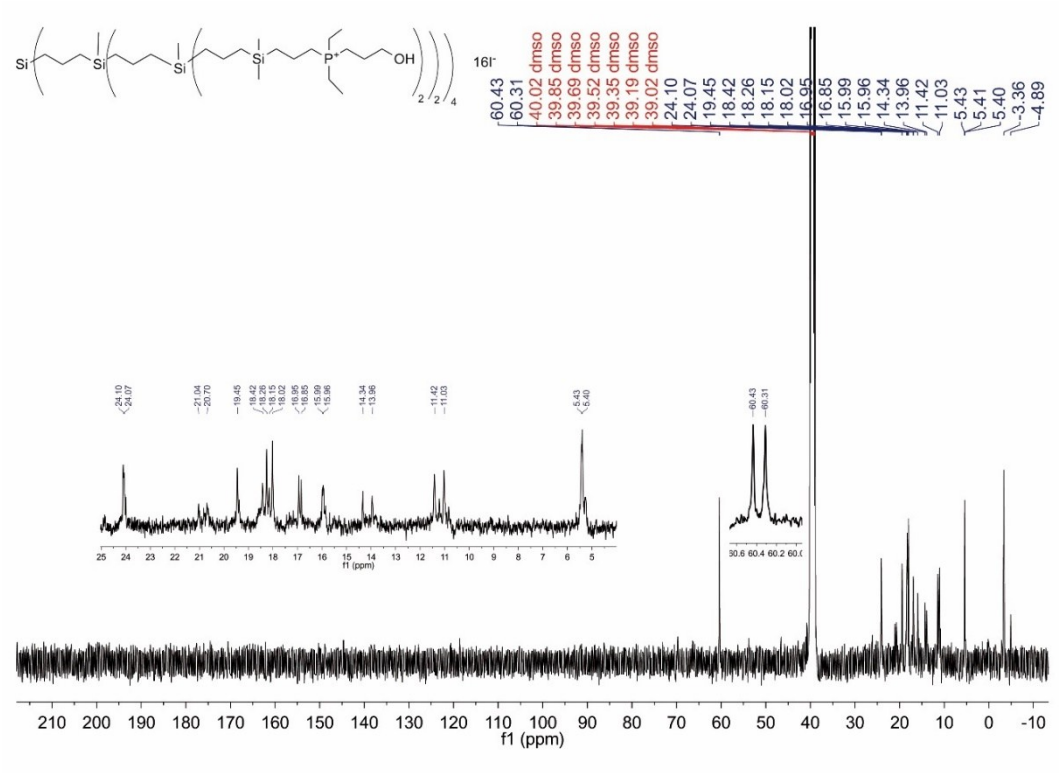

Figure SI31. ^{13}C {H} NMR (125 MHz, DMSO-*d6*) of **15**.

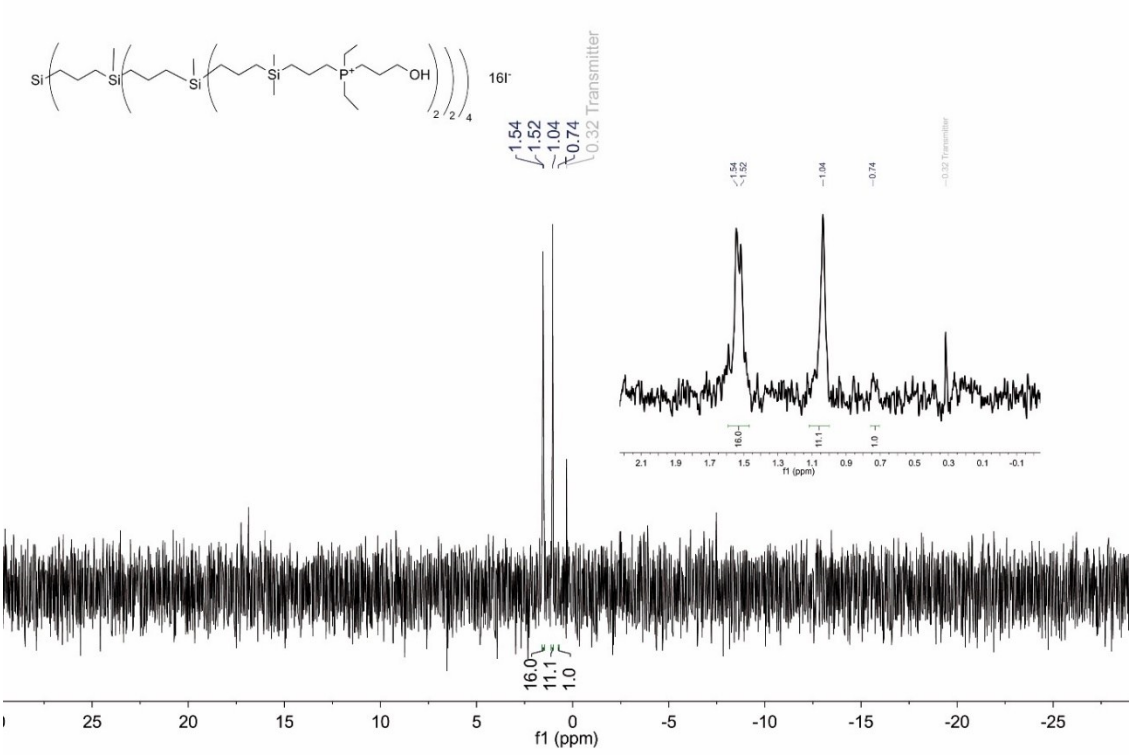

Figure SI32. ^{29}Si {H} NMR (99 MHz, DMSO-*d6*) of **15**.

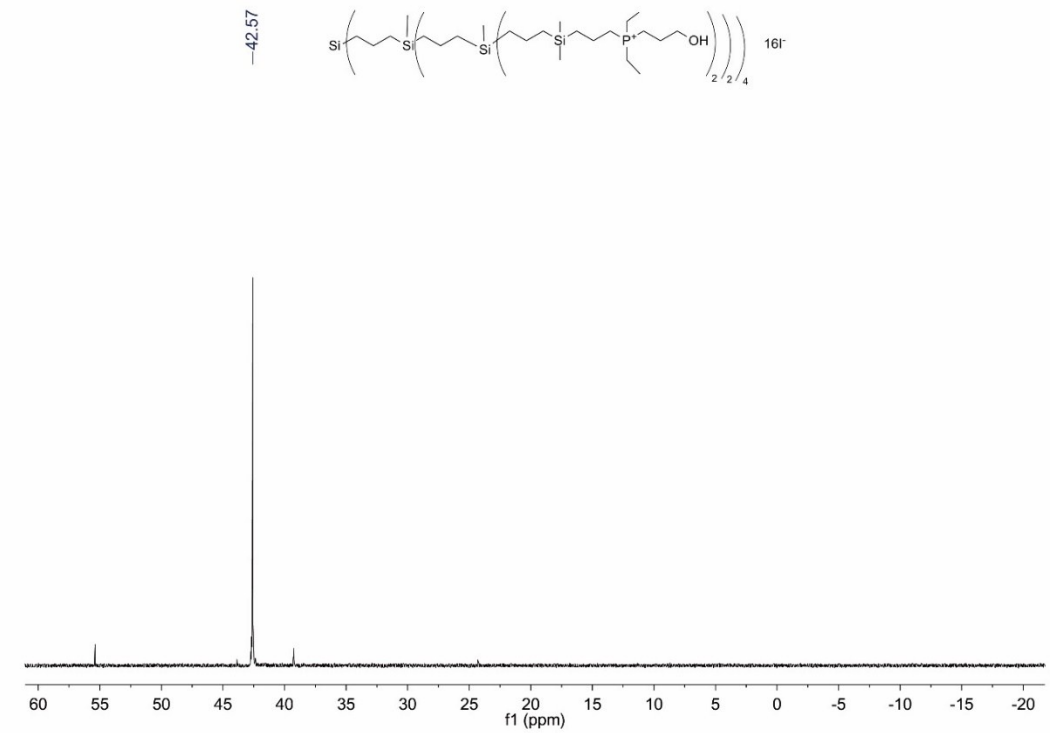

Figure SI33. $^{31}P\{H\}$ NMR (121 MHz, DMSO-*d6*) of **15**.

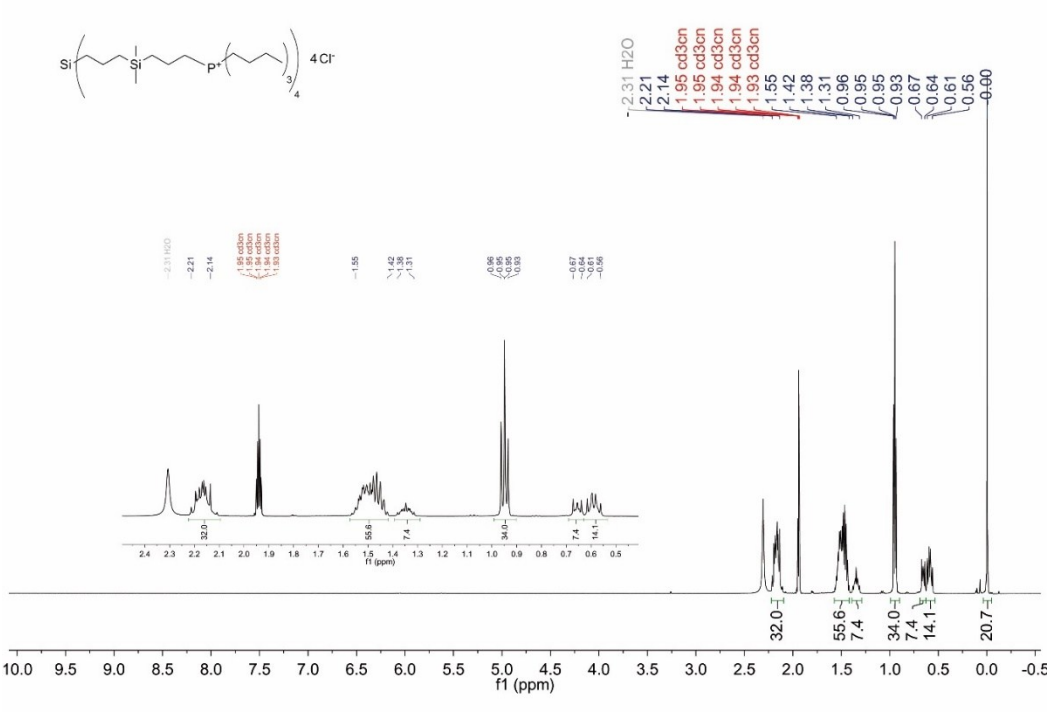

Figure SI34. ^{1}H NMR (500 MHz, CD_3CN) of **19**.

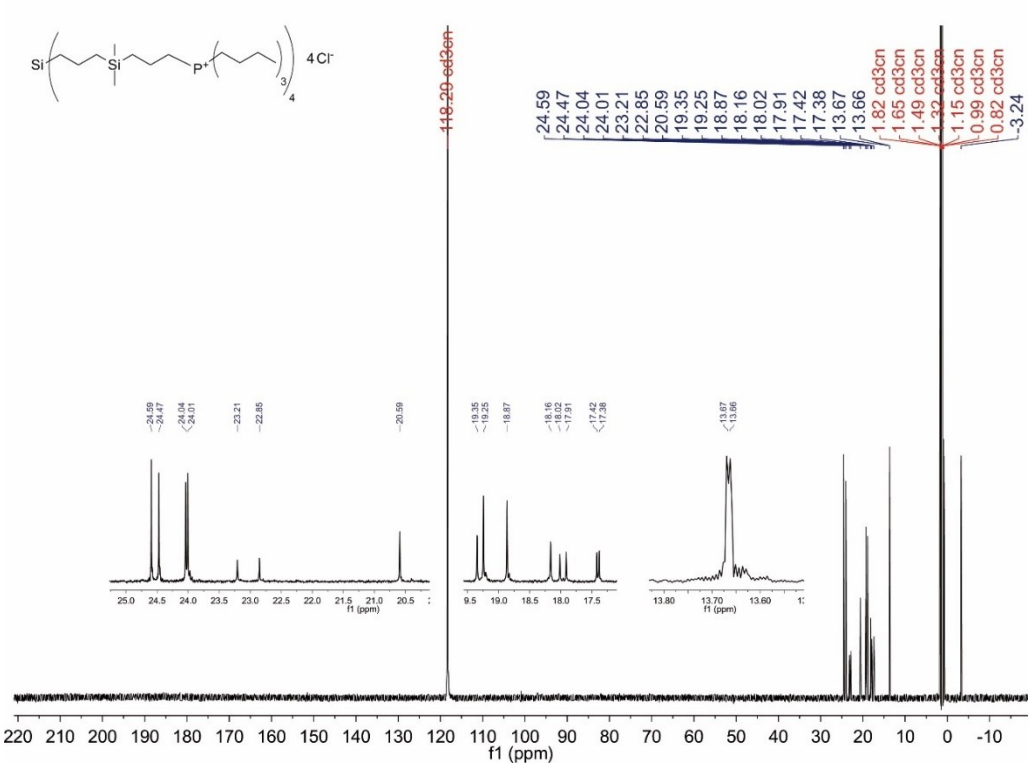

Figure SI35. ^{13}C {H} NMR (125 MHz, CD_3CN) of **19**.

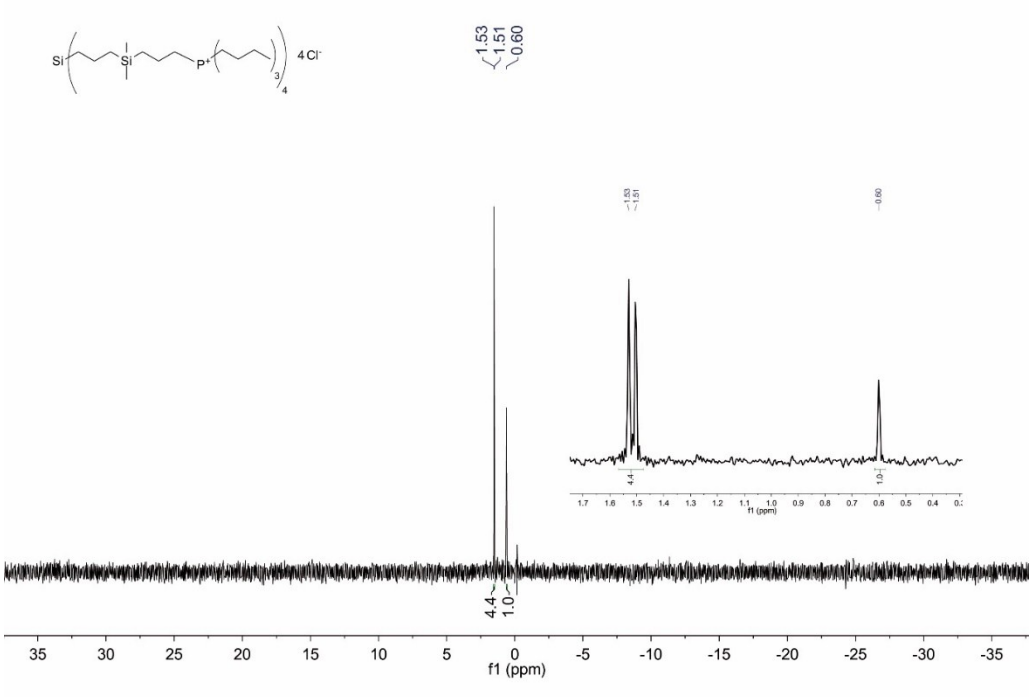

Figure SI36. ^{29}Si {H} NMR (99 MHz, CD_3CN) of **19**.

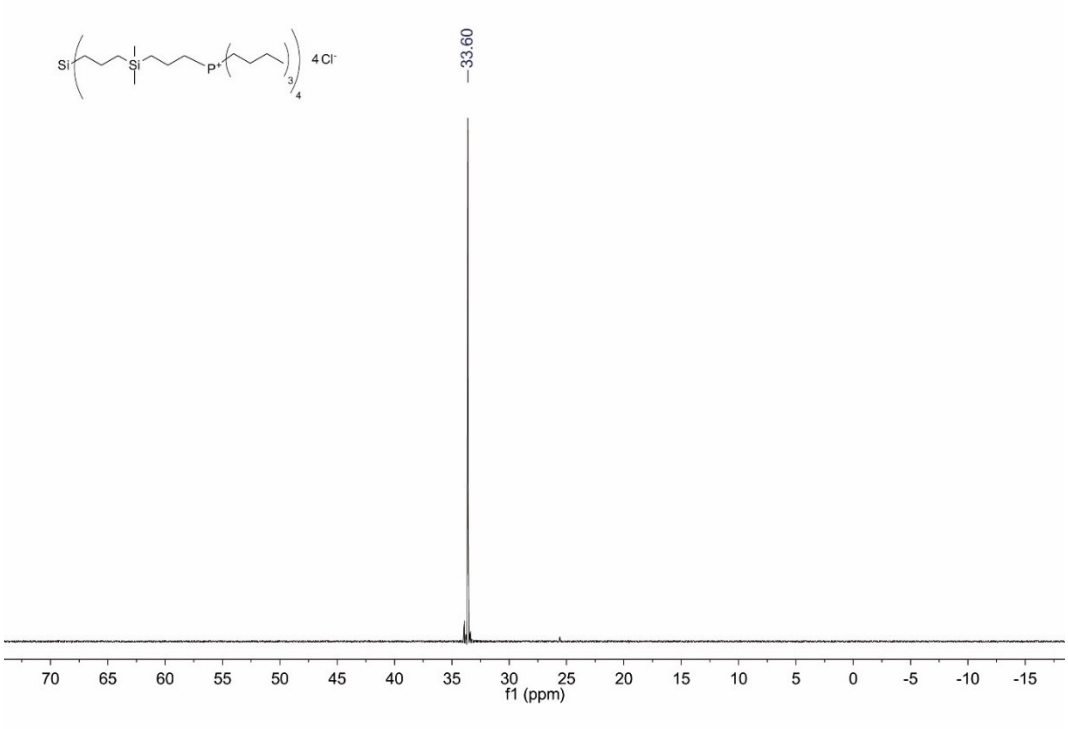

Figure SI37. $^{31}P\{H\}$ NMR (121 MHz, CD_3CN) of **19**.

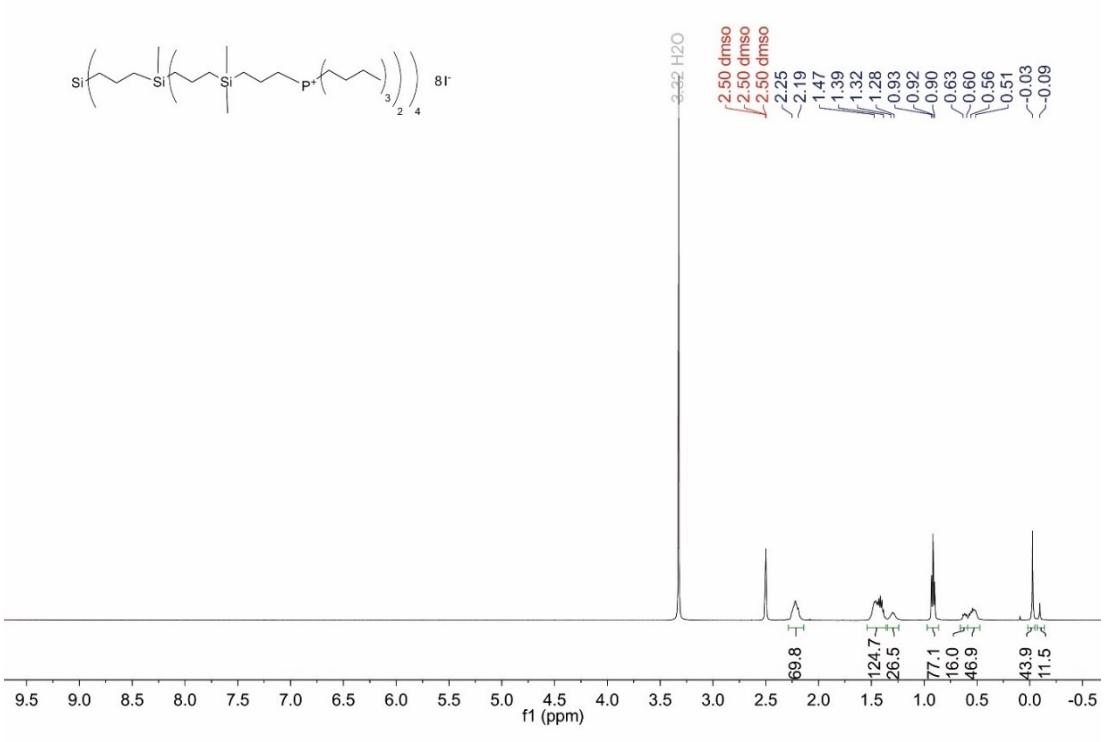

Figure SI38. ^{1}H NMR (500 MHz, DMSO-*d6*) of **17**.

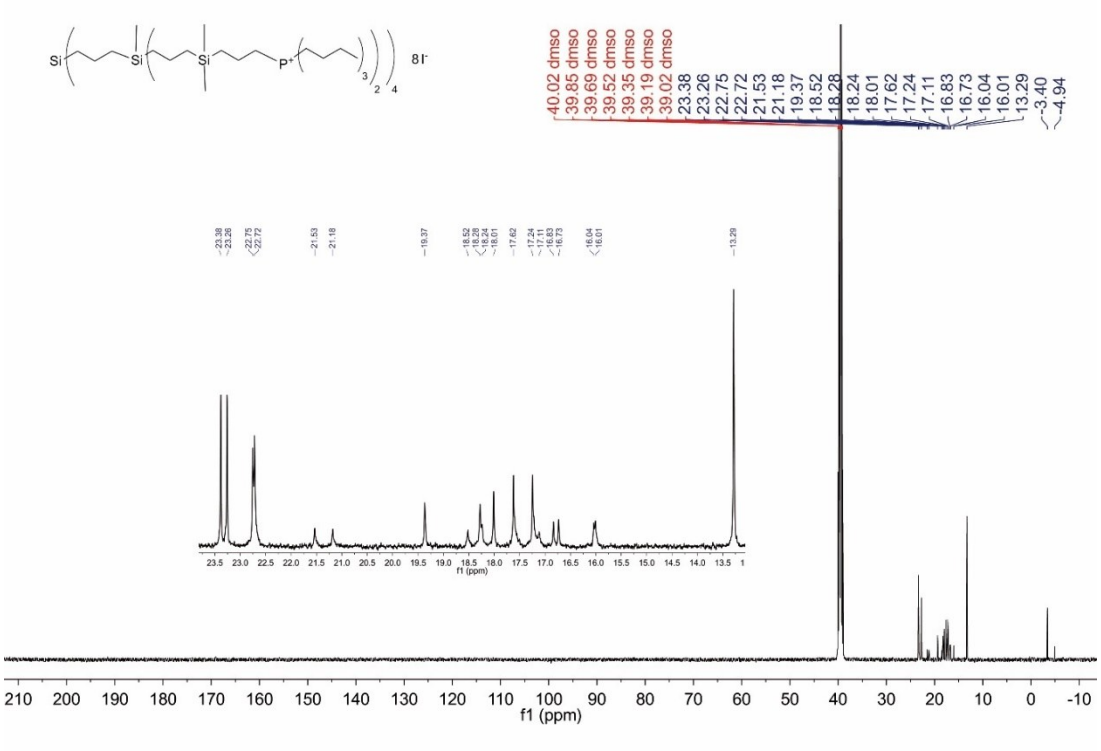

Figure SI39. 13C {H} NMR (125 MHz, DMSO-d6) of 17.

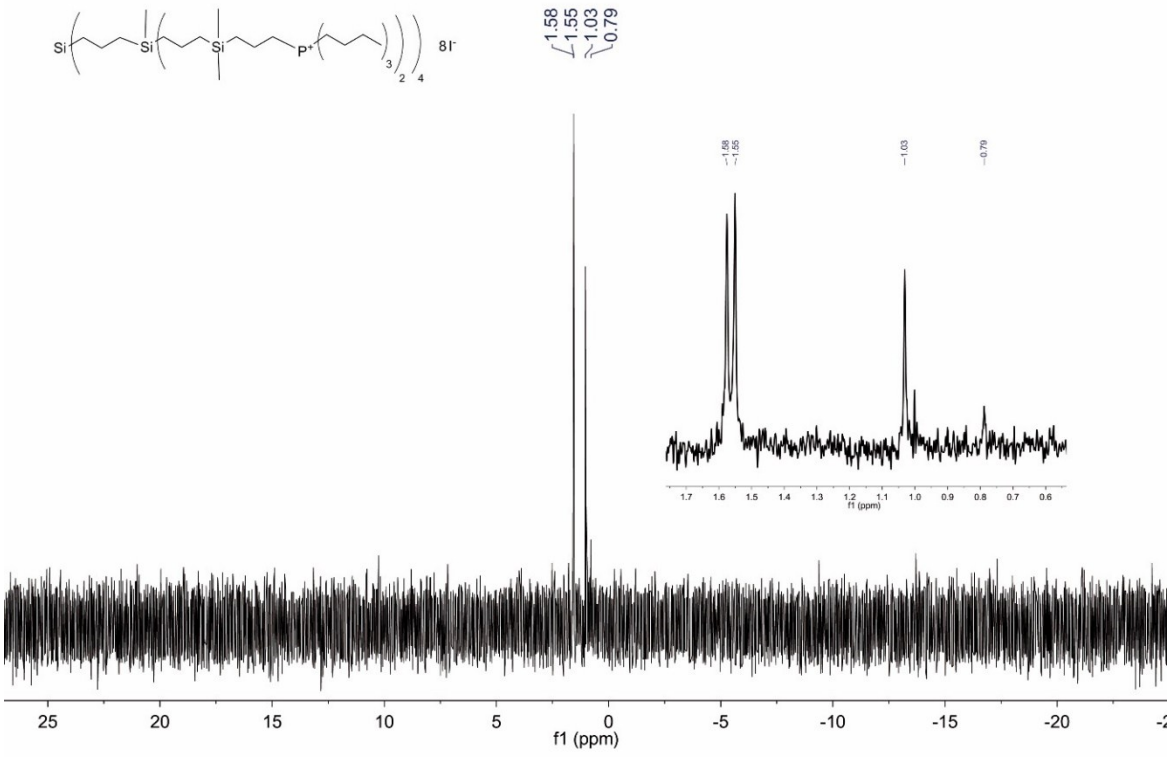

Figure SI40. ^{29}Si Inept {H} NMR (99 MHz, DMSO-*d6*) of **17**.

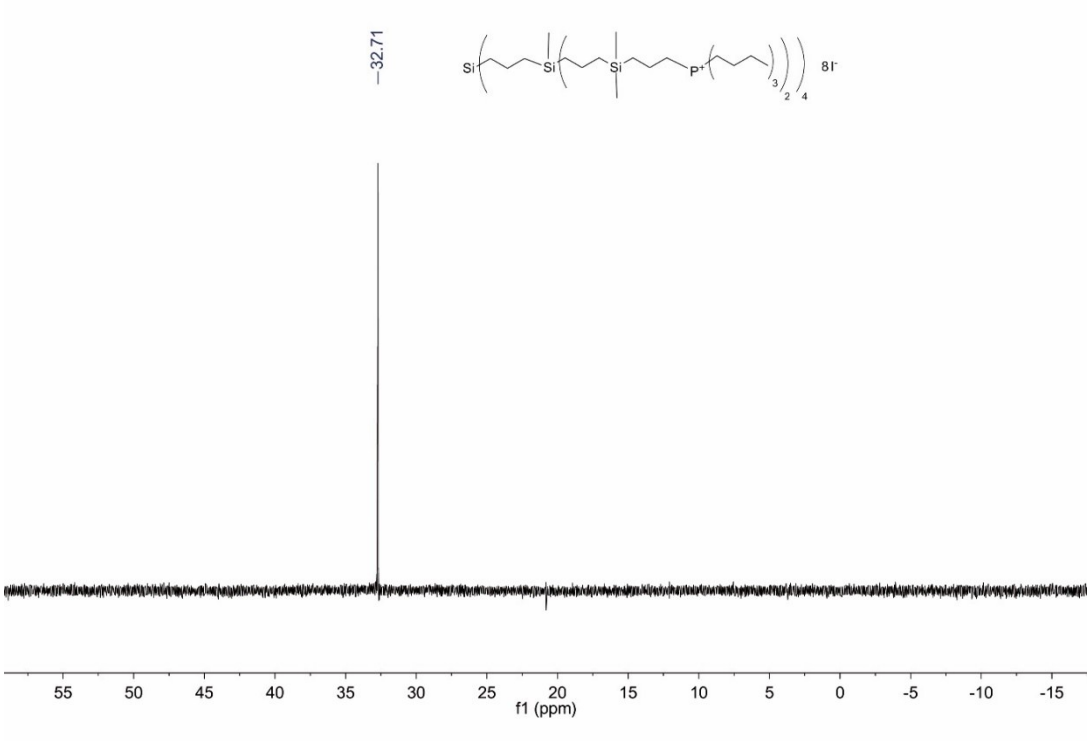

Figure SI41. $^{31}P\{H\}$ NMR (202 MHz, DMSO-*d6*) of **17**.

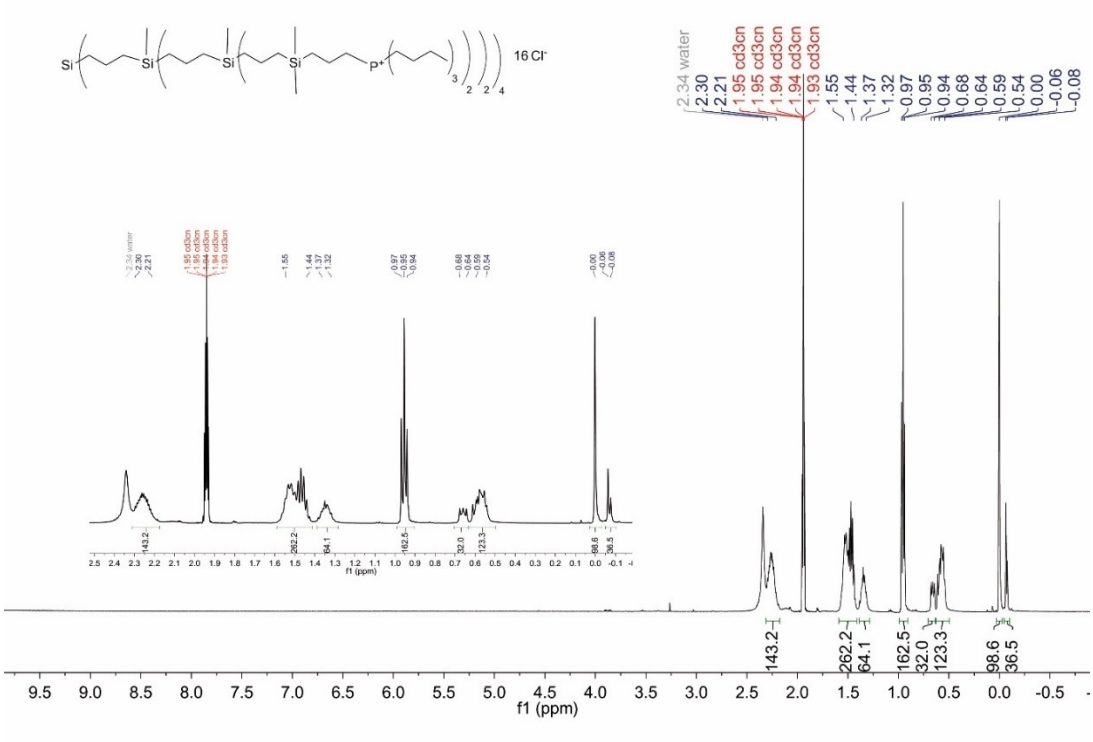

Figure SI42. ^{1}H NMR (500 MHz, CD_3CN) of **21**.

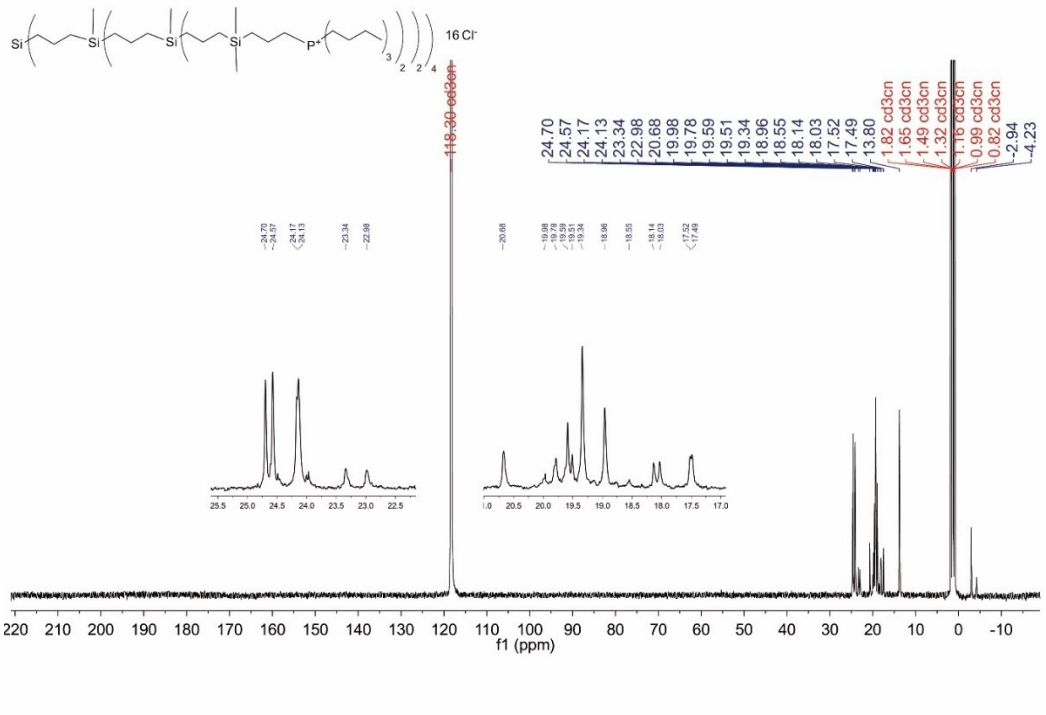

Figure SI43. ^{13}C {H} NMR (125 MHz, CD_3CN) of **21**.

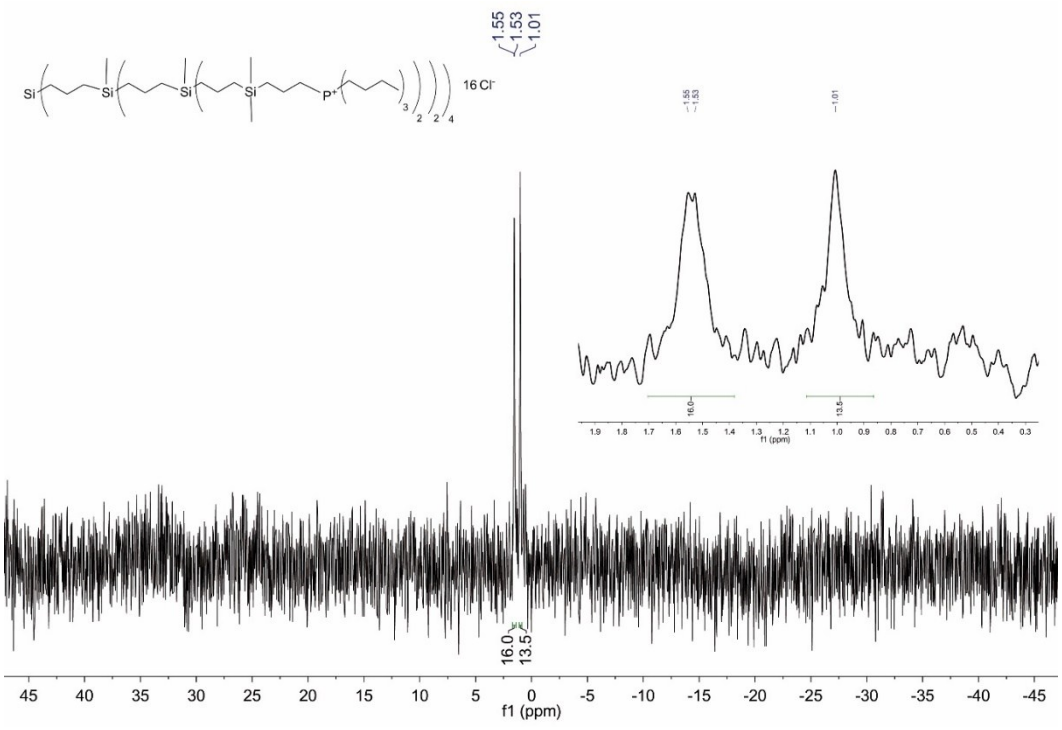

Figure SI44. ^{29}Si Inept {H} NMR (59 MHz, CD_3CN) of **21**.

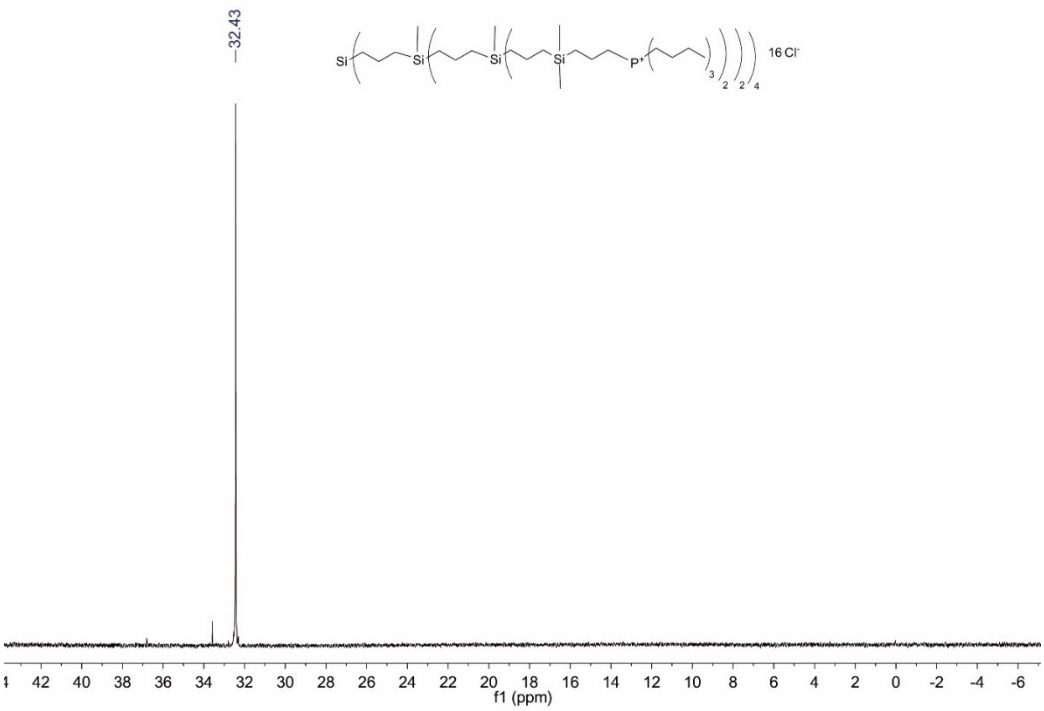

Figure SI45. $^{31}P\{H\}$ NMR (202 MHz, CD_3CN) of **21**.

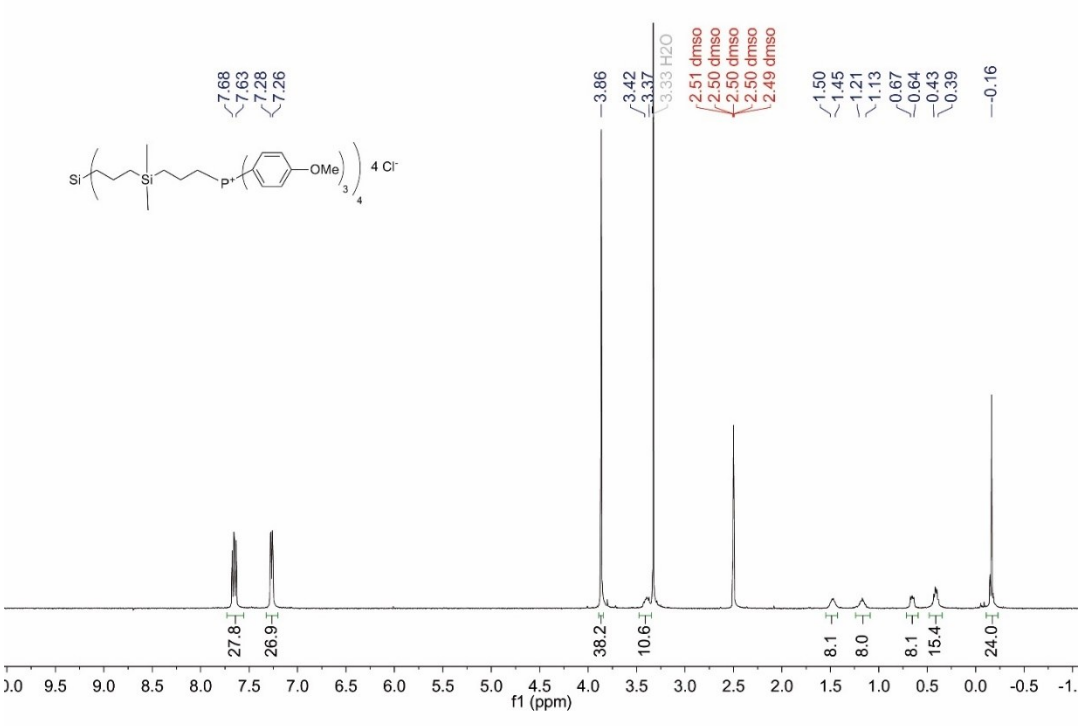

Figure SI46. ^{1}H NMR (500 MHz, DMSO-*d6*) of **25**.

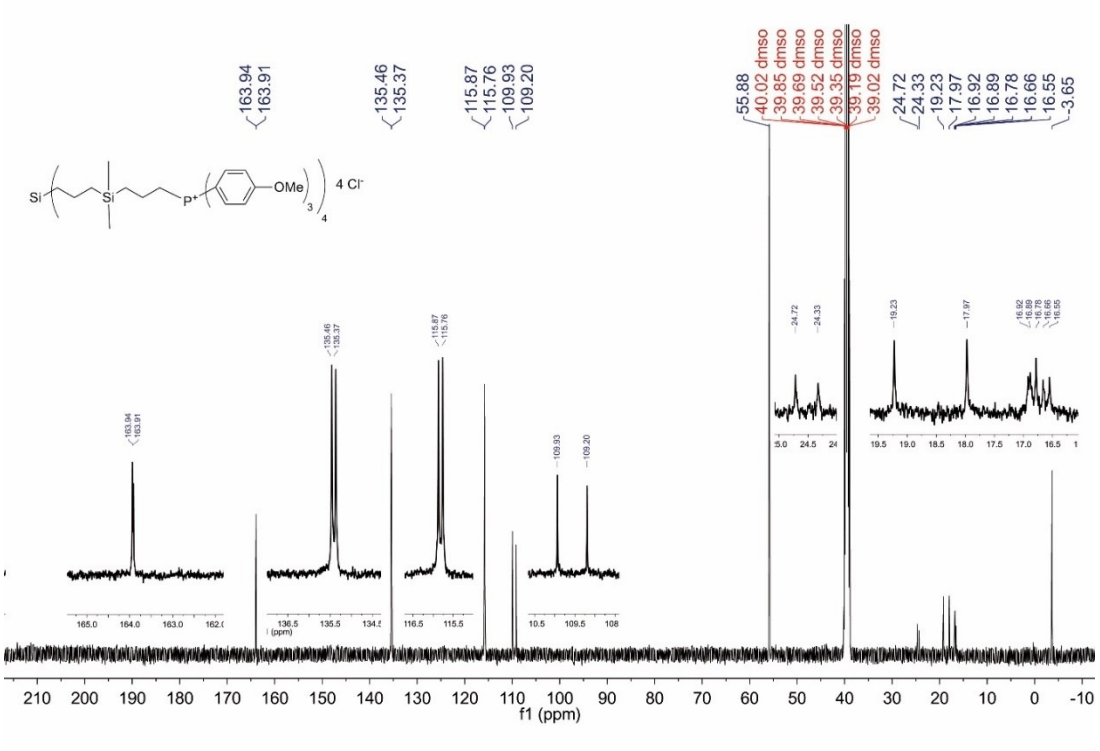

Figure SI47. ^{13}C {H} NMR (125 MHz, DMSO-*d6*) of **25**.

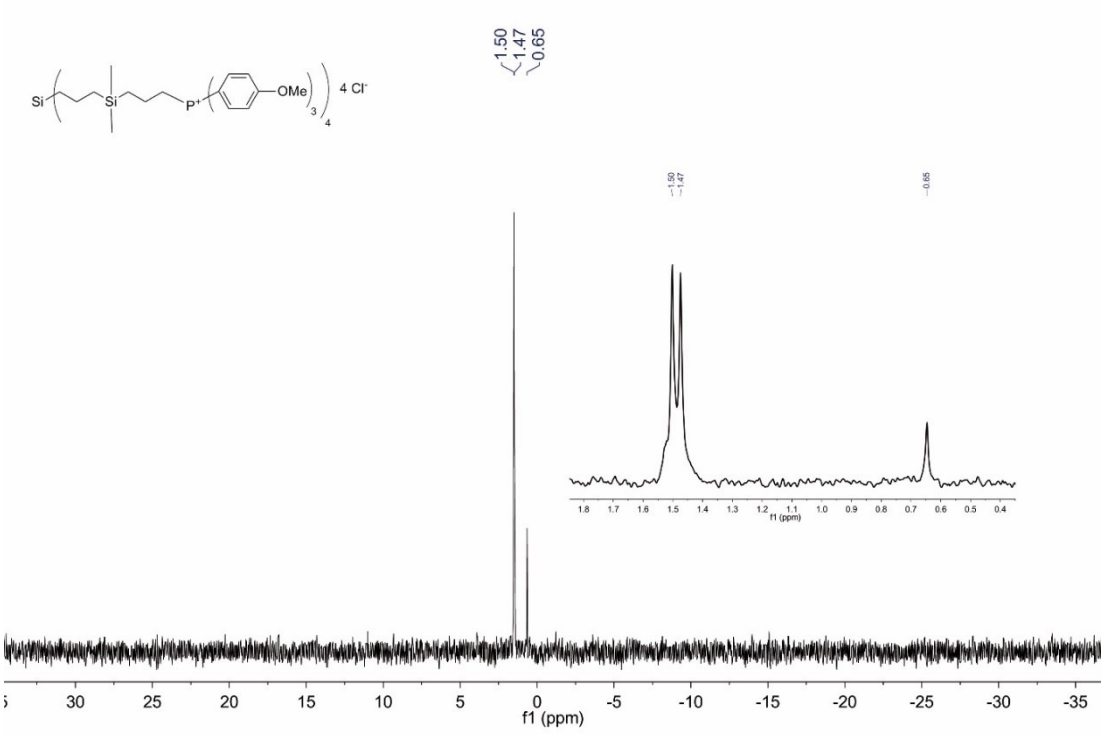

Figure SI48. ^{29}Si Inept {H} NMR (99 MHz, DMSO-*d6*) of **25**.

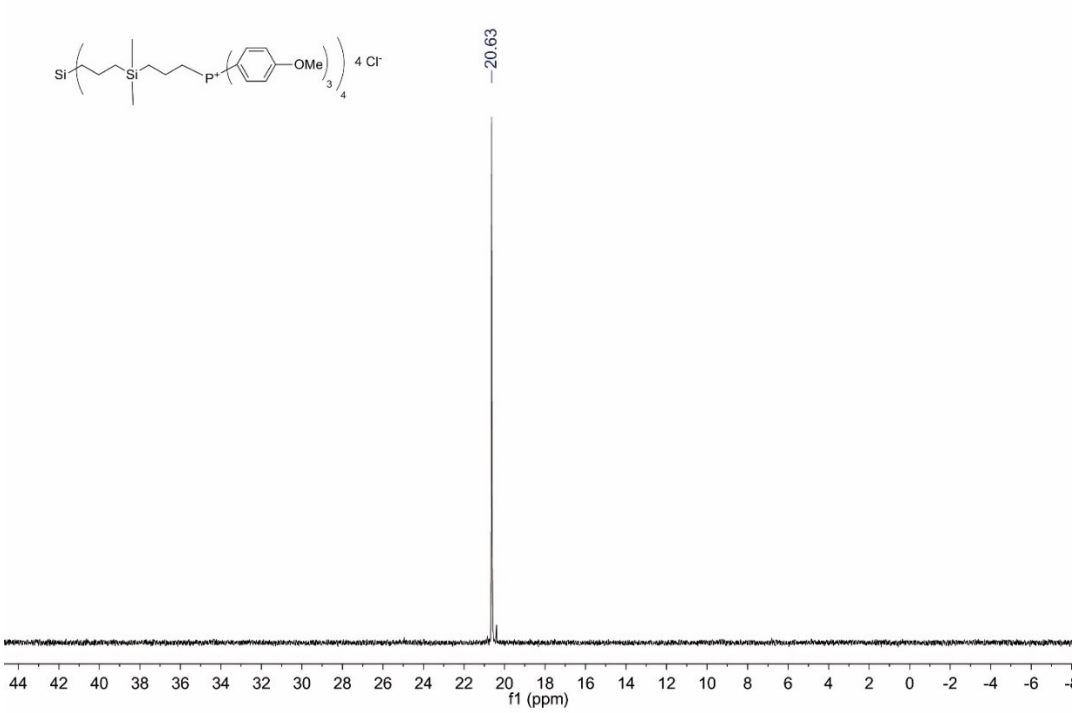

Figure SI49. $^{31}P\{H\}$ NMR (202 MHz, DMSO-*d6*) of **25**.

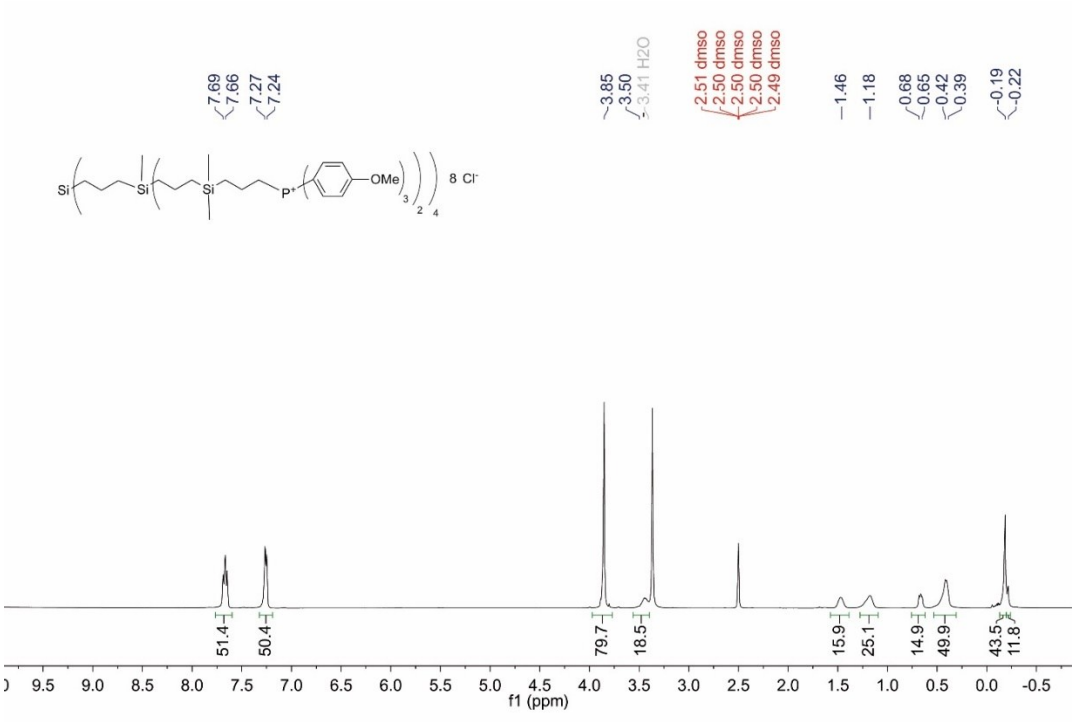

Figure SI50. ^{1}H NMR (500 MHz, DMSO-*d6*) of **26**.

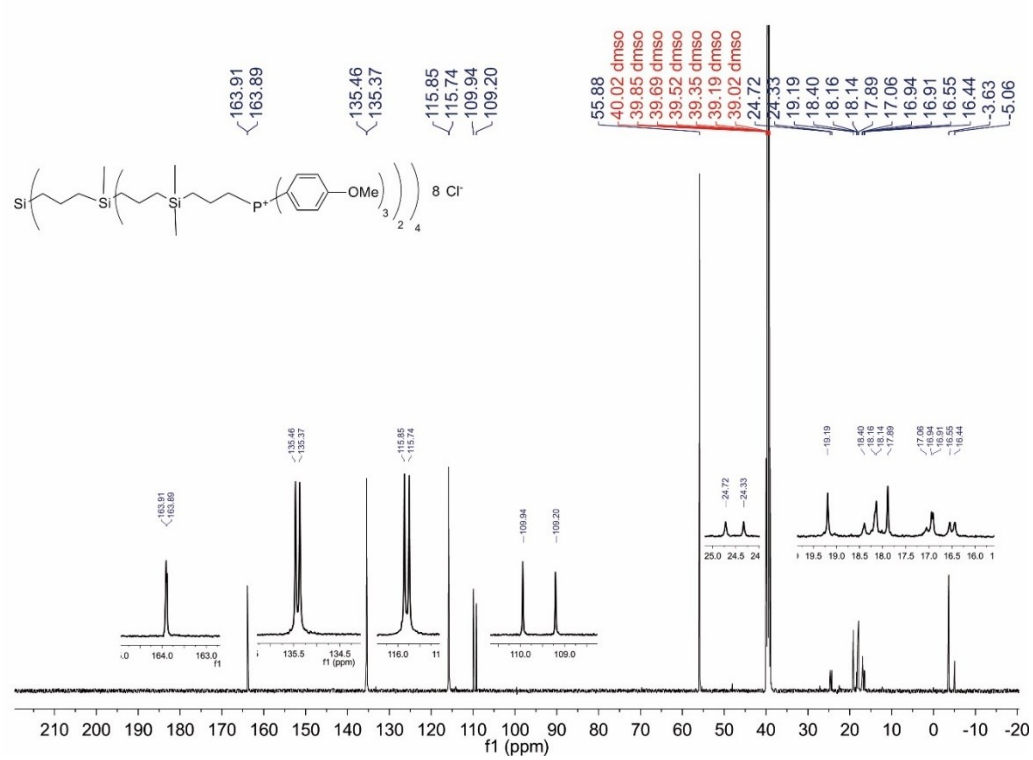

Figure SI51. ^{13}C {H} NMR (125 MHz, DMSO-*d6*) of **26**.

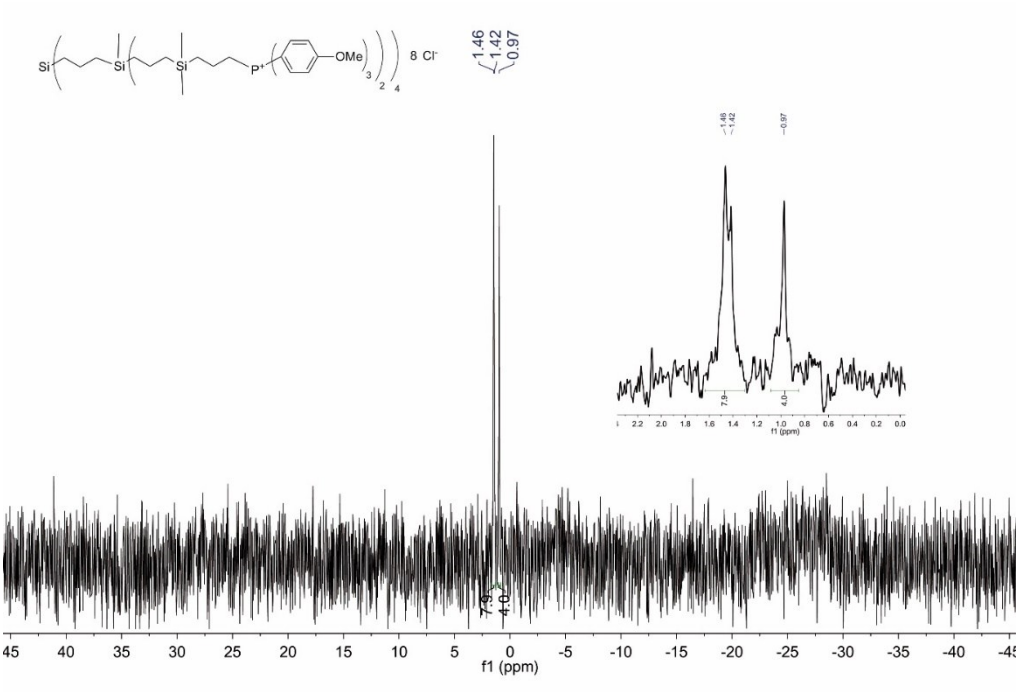

Figure SI52. ^{29}Si {H} NMR (59 MHz, DMSO-*d6*) of **26**.

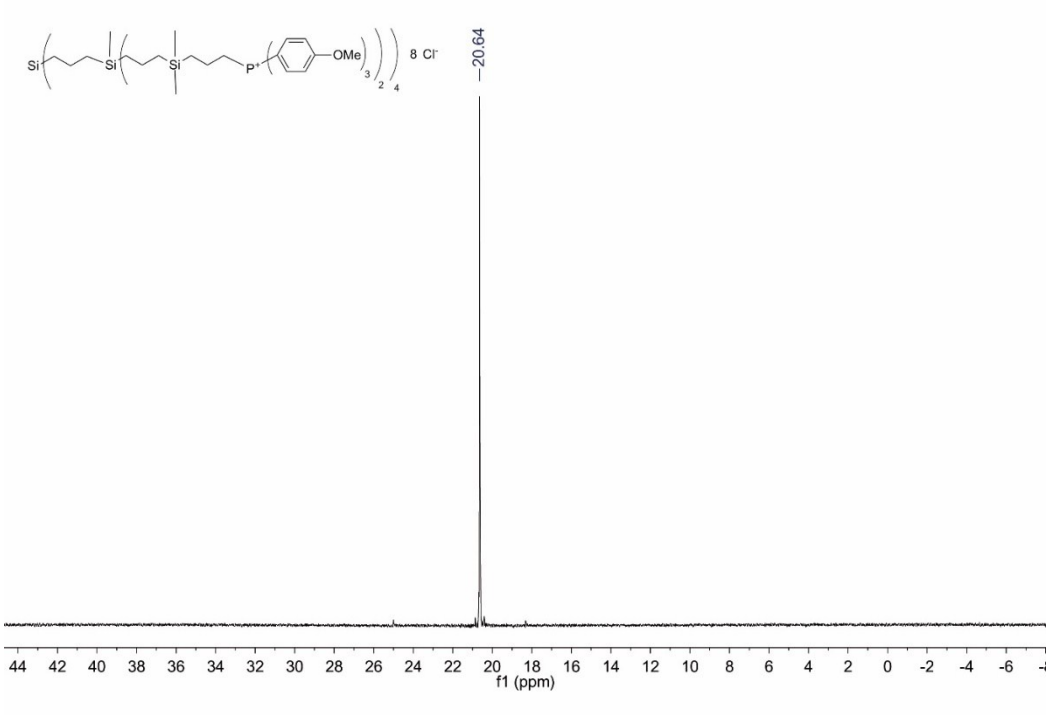

Figure SI53. $^{31}P\{H\}$ NMR (202 MHz, DMSO-*d6*) of **26**.

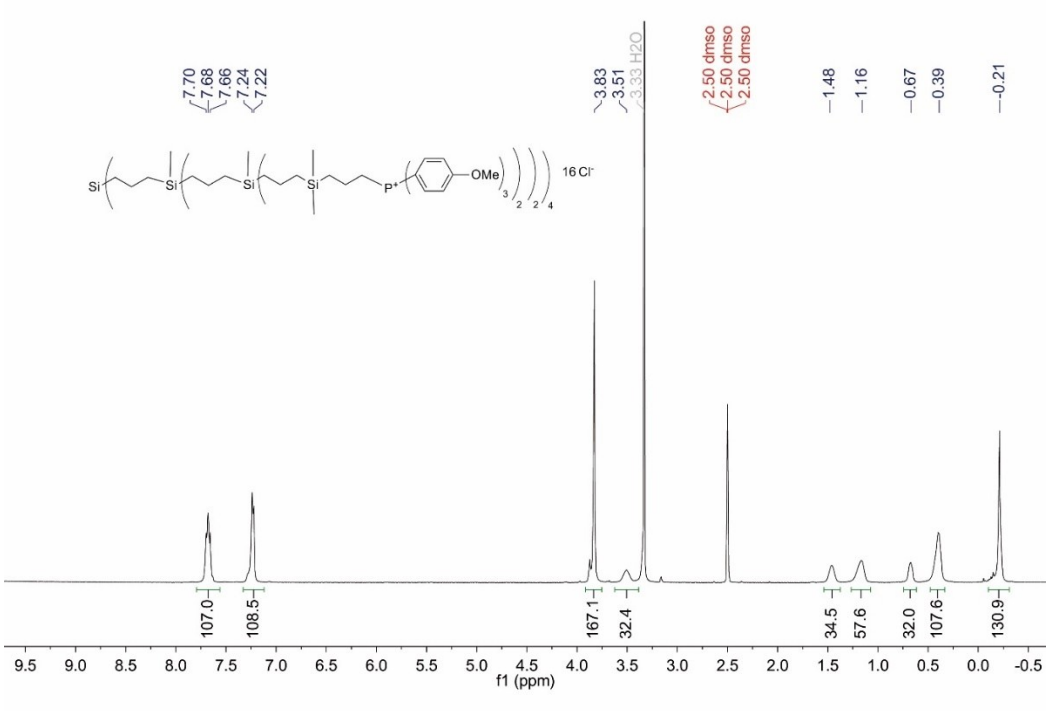

Figure SI54. ^{1}H NMR (500 MHz, DMSO-*d6*) of **27**.

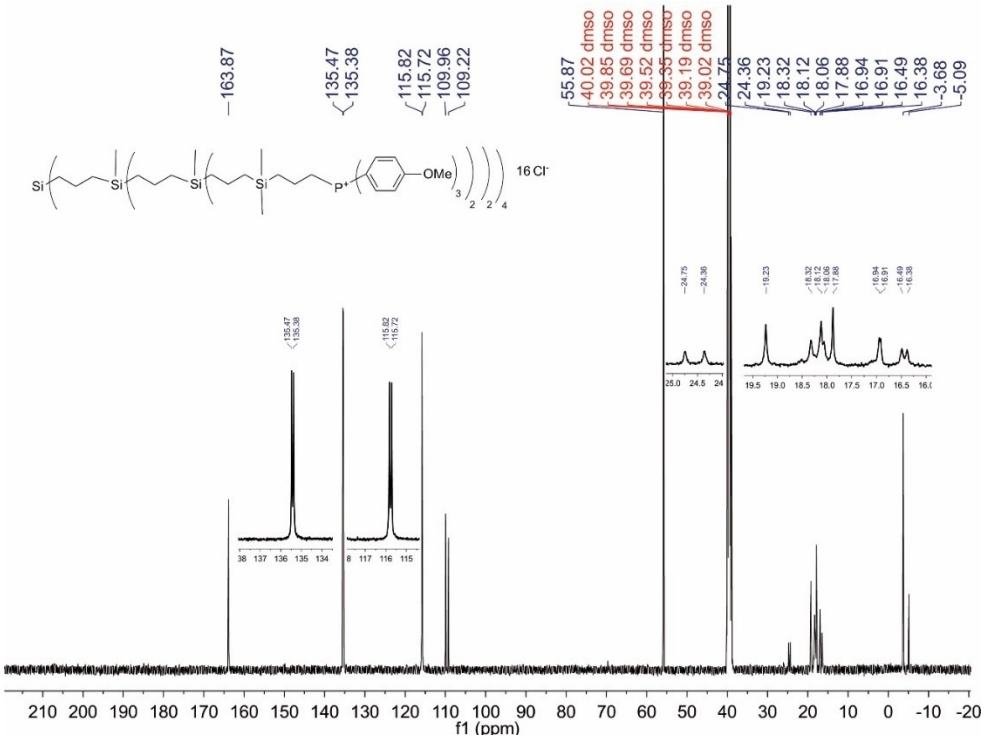

Figure SI55. ^{13}C {H} NMR (125 MHz, DMSO-*d6*) of **27**.

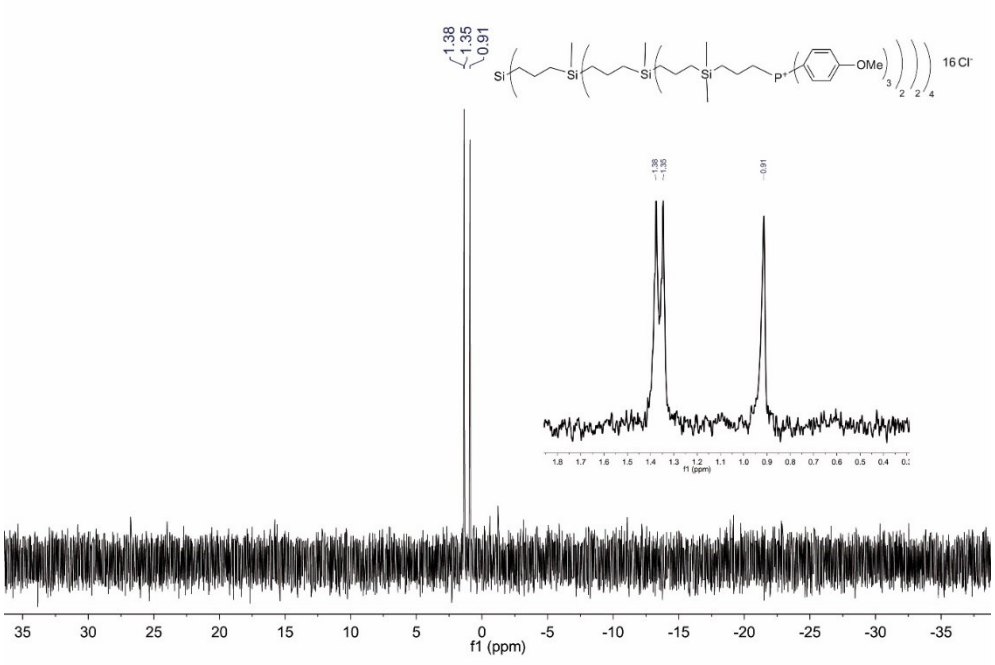

Figure SI56. ^{29}Si Inept {H} NMR (99 MHz, DMSO-*d6*) of **27**.

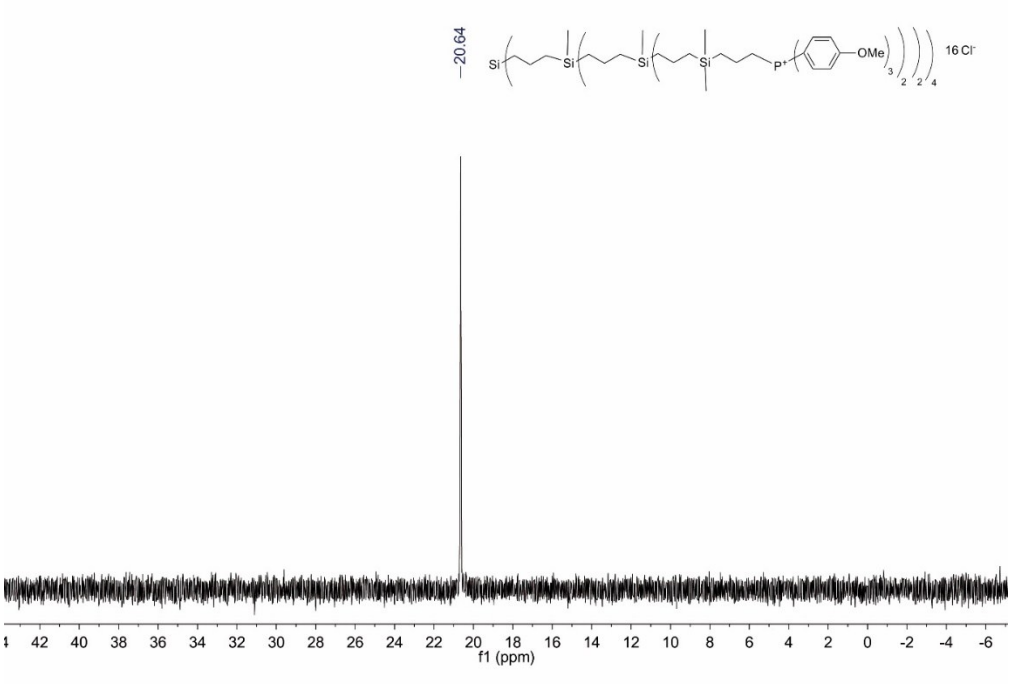

Figure SI57. $^{31}P\{H\}$ NMR (202 MHz, DMSO-*d6*) of **27**.

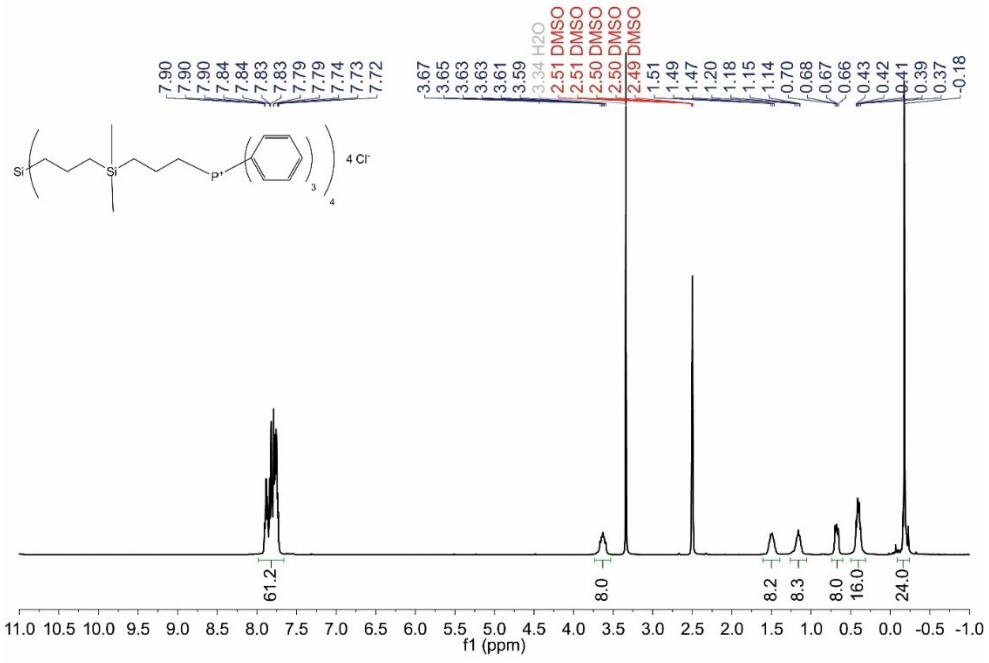

Figure SI58. ^{1}H NMR (400 MHz, DMSO-*d6*) of **31**.

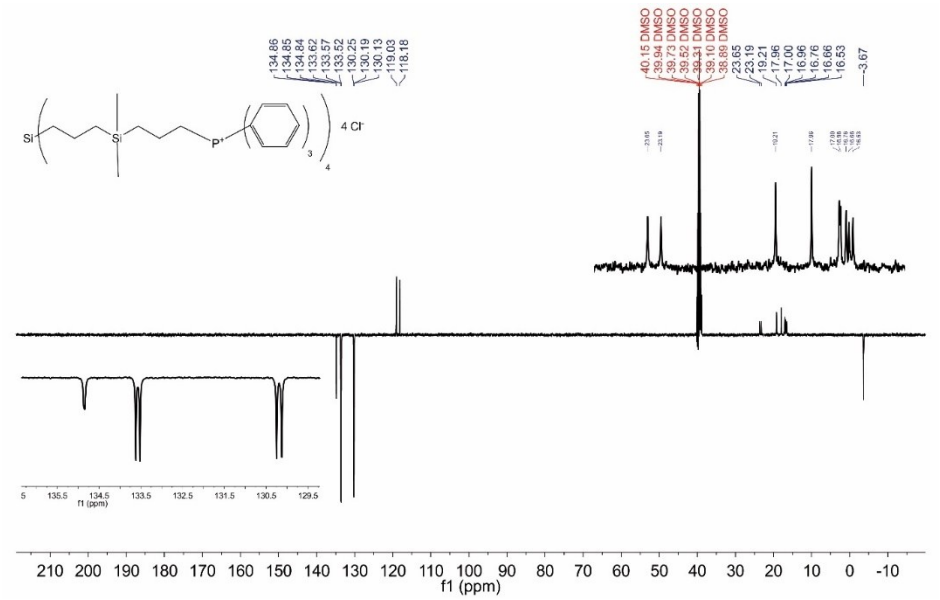

Figure SI59. APT NMR (100 MHz, DMSO-*d6*) of **31**.

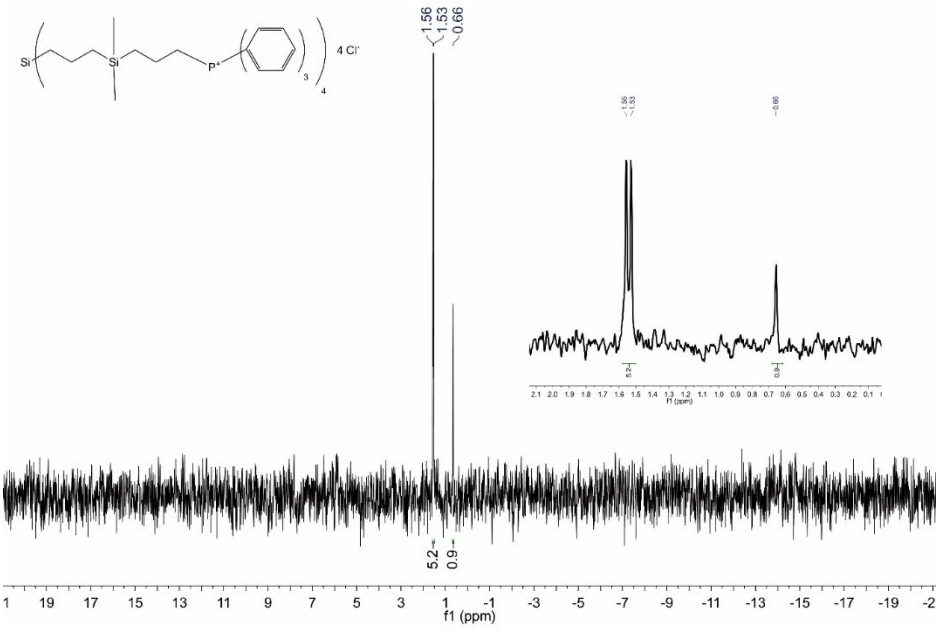

Figure SI60. ^{29}Si {^{1}H} NMR (99 MHz, DMSO-*d6*) of **31**.

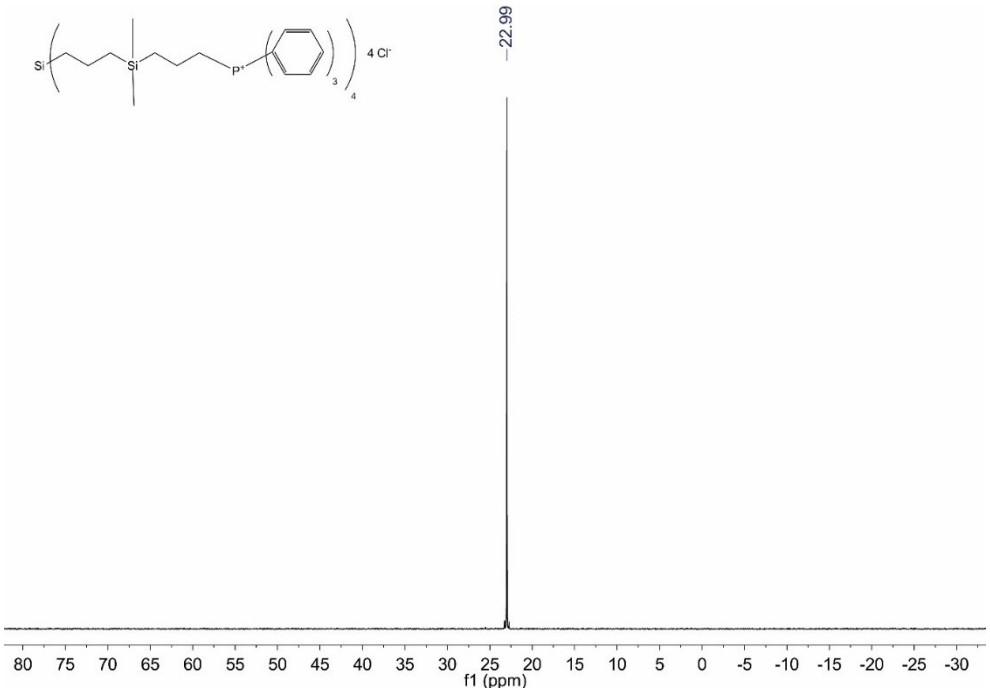

Figure SI61. $^{31}P\{^{1}H\}$ NMR (161 MHz, DMSO-*d6*) of **31**.

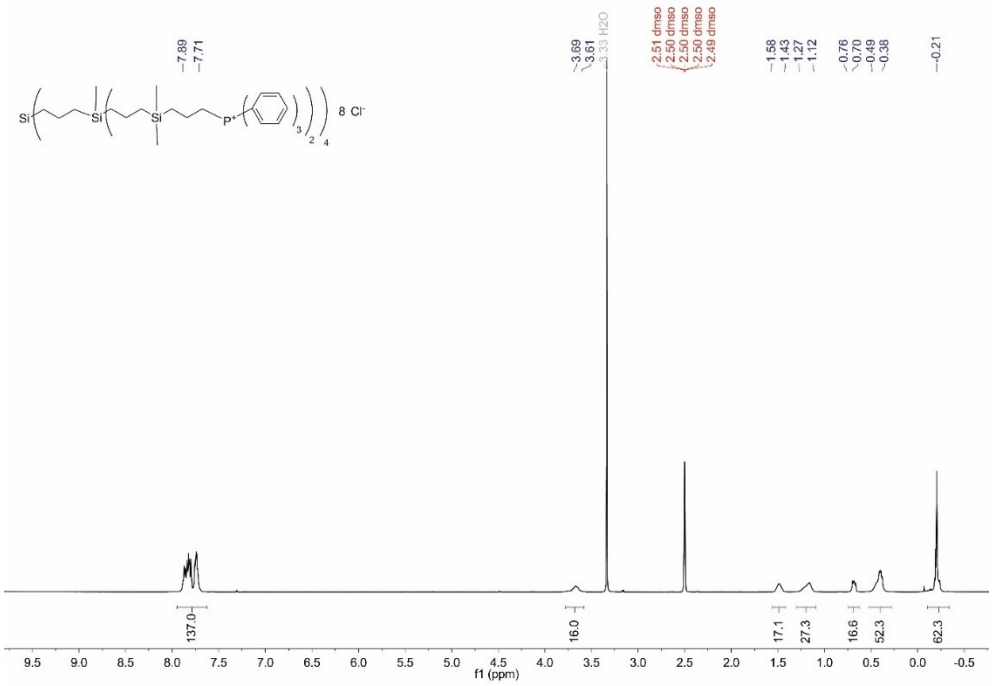

Figure SI62. ^{1}H NMR (499 MHz, DMSO-*d6*) of **32**.

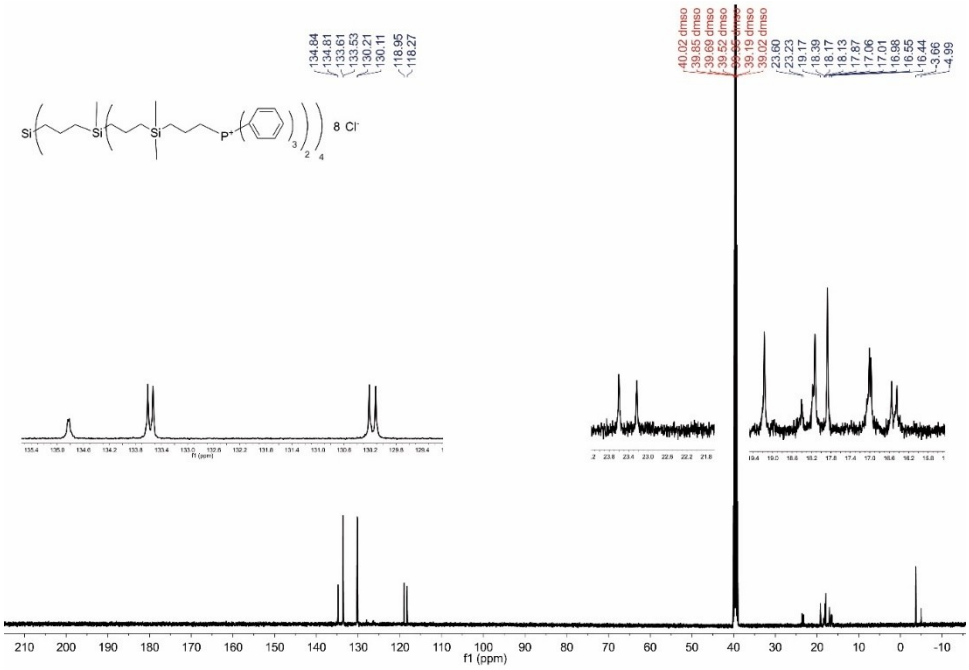

Figure SI63. $^{13}C\{^{1}H\}$ NMR (125 MHz, DMSO-*d6*) of **32**.

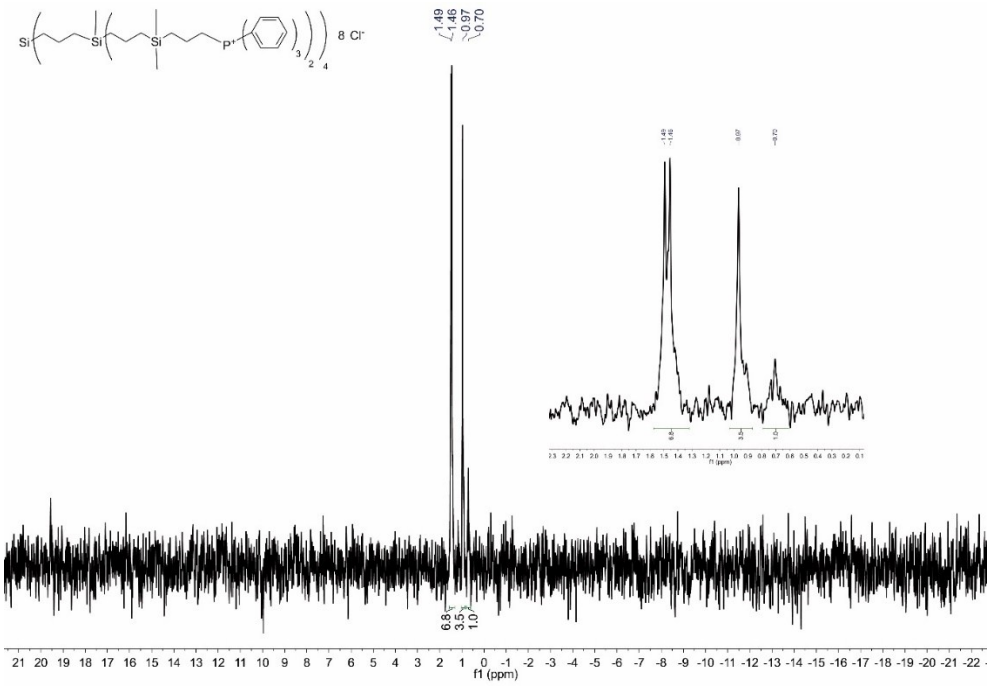

Figure SI64. $^{29}Si\ \{^{1}H\}$ NMR (79 MHz, DMSO-*d6*) of **32**.

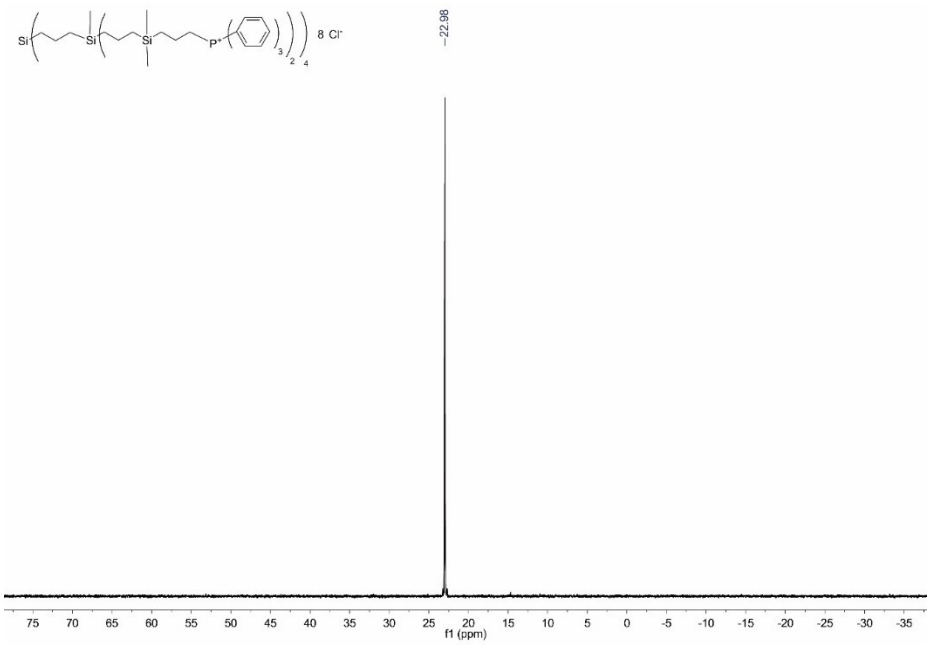

Figure SI65. $^{31}P\{^{1}H\}$ NMR (161 MHz, DMSO-*d6*) of **32**.

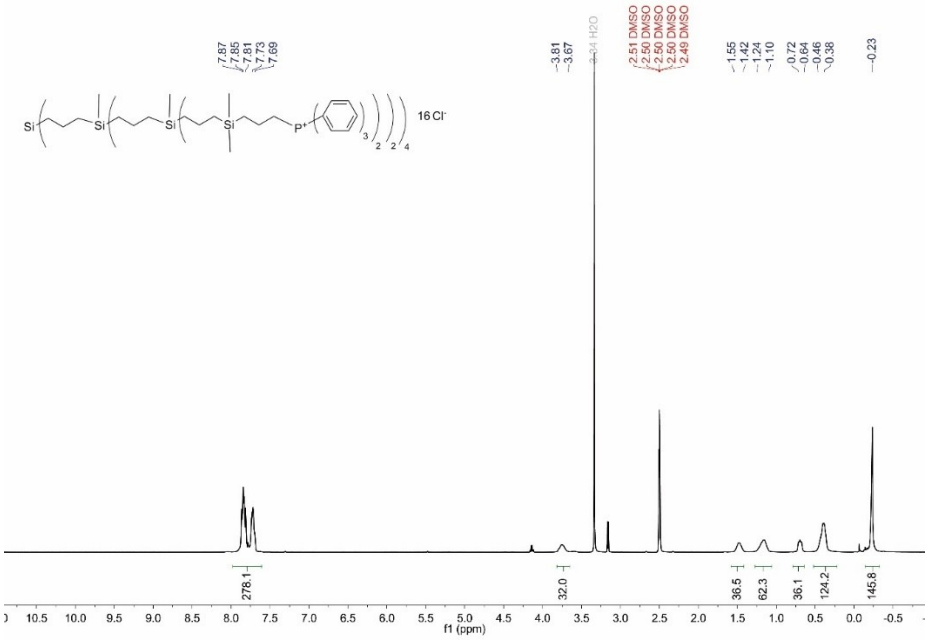

Figure SI66. ^{1}H NMR (400 MHz, DMSO-*d6*) of **33**.

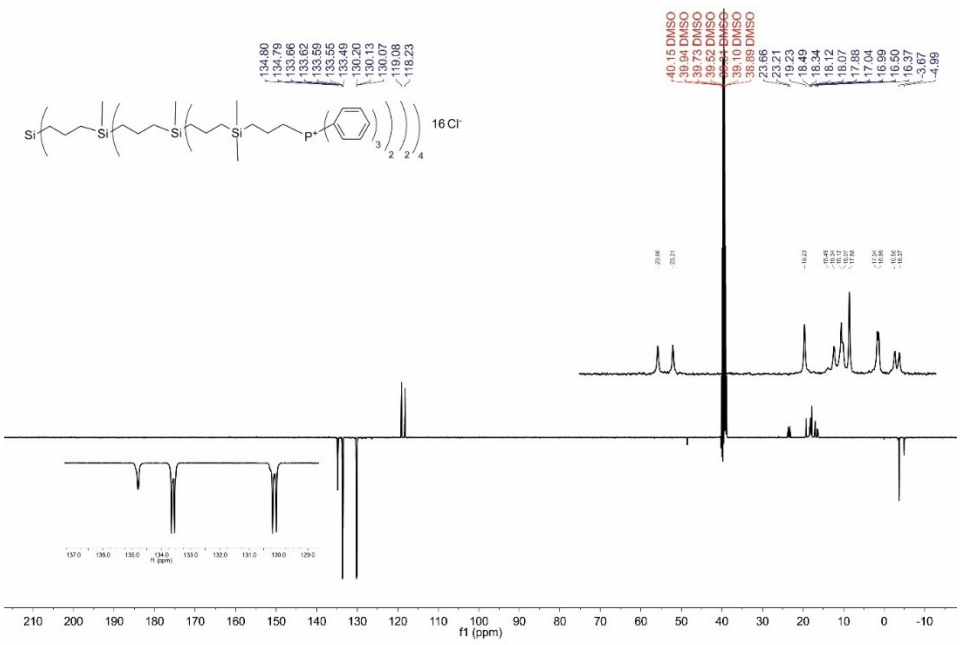

Figure SI67. APT NMR (100 MHz, DMSO-*d6*) of **33**.

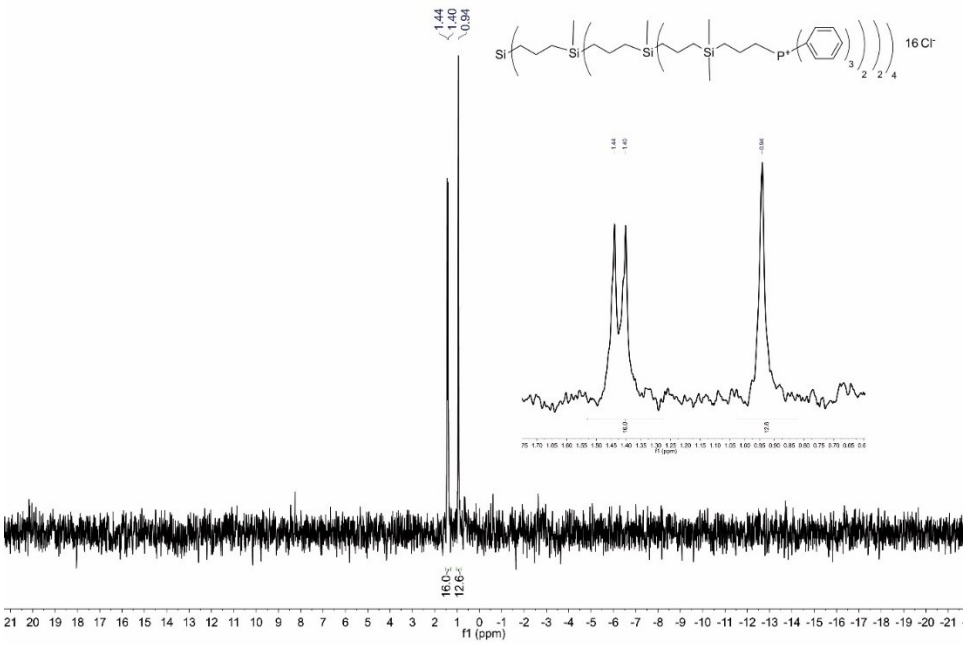

Figure SI68. ^{29}Si {^{1}H} NMR (79 MHz, DMSO-*d6*) of **33**.

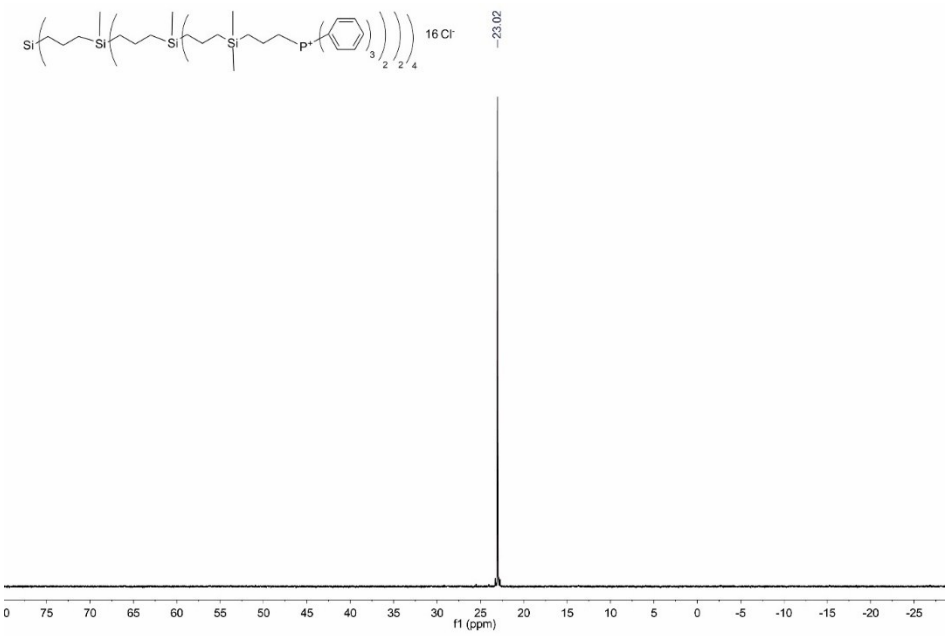

Figure SI69. $^{31}P\{^{1}H\}$ NMR (161 MHz, DMSO-*d6*) of **33**.

Table SI1. ESI HRMS of compound 31.

	Molecular formula: $[C_{104}H_{132}P_4Si_5Cl_4]$
$[M - 2Cl^-]^{2+}$ calc. 858.3753	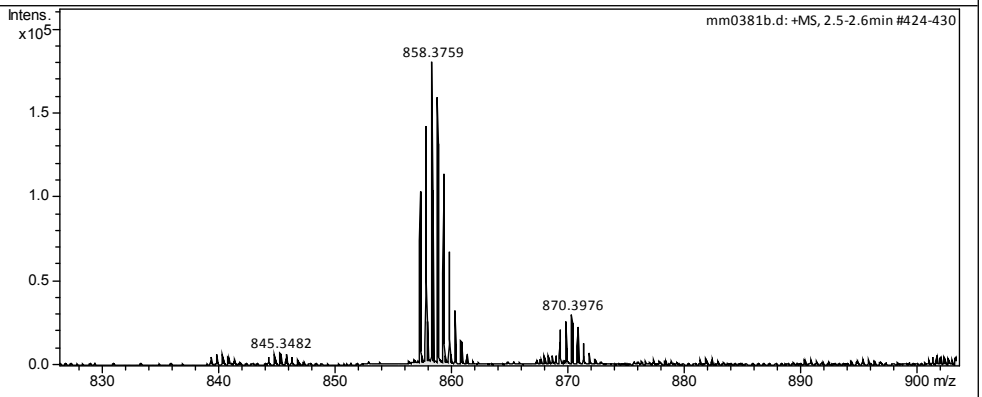
$[M - 3Cl^-]^{3+}$ calc. 560.5941	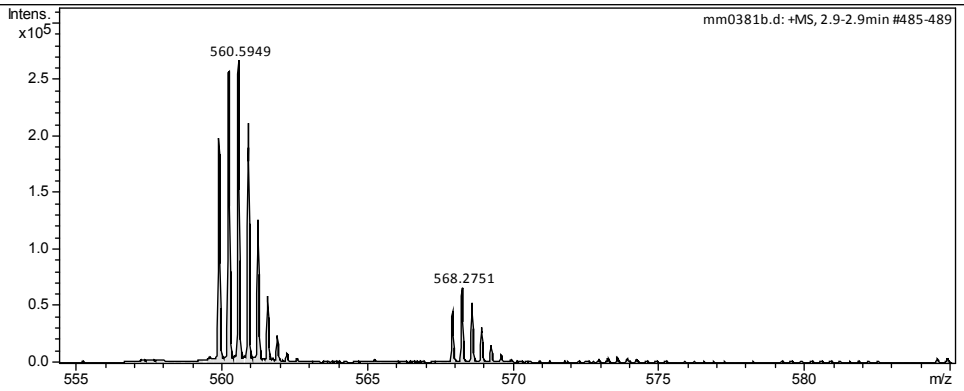
$[M - 4Cl^-]^{4+}$ calc. 411.4532	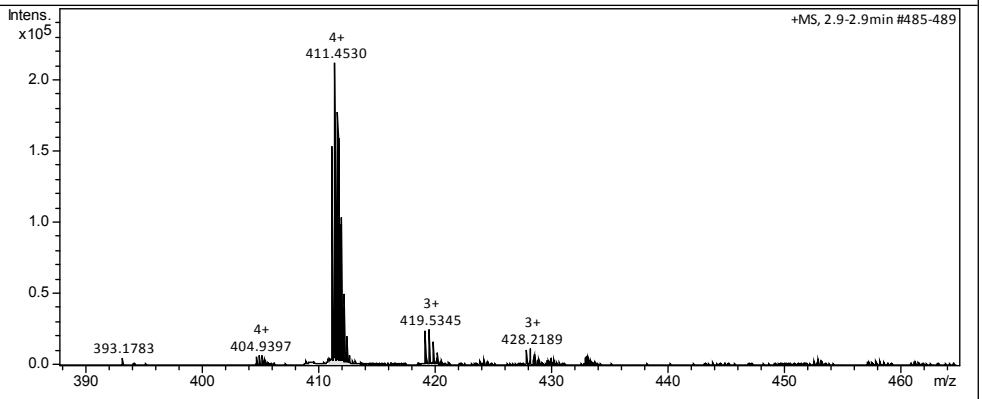

Table SI2. **ESI HRMS of compound 32**.

	Molecular formula: $C_{224}H_{300}P_8Si_{13}Cl_8$
$[M - 2Cl^-]^{2+}$ Calc. 1908.8261, 2+	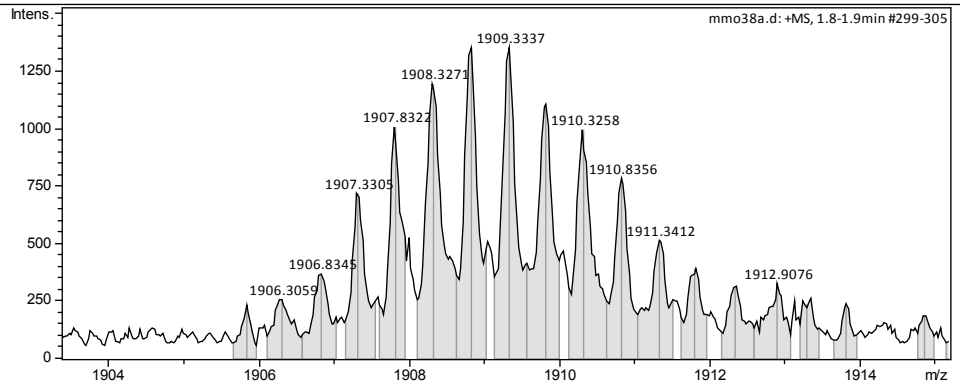
$[M - 3Cl^-]^{3+}$ Calc.1260.8945	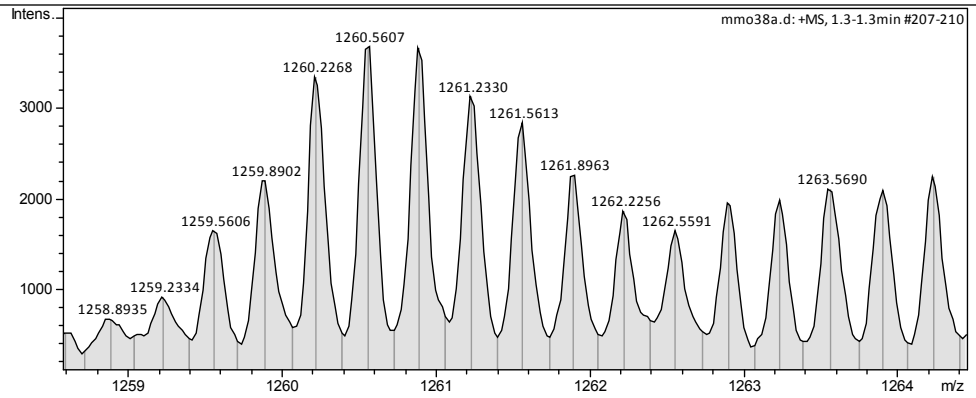
$[M - 4Cl^-]^{4+}$ Calc. 936.6787	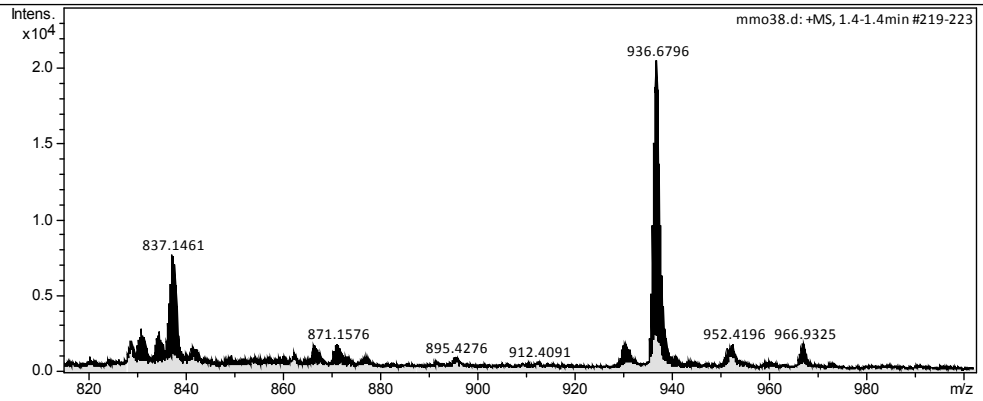

$[M - 5Cl^-]^{5+}$ Calc. 742.3492	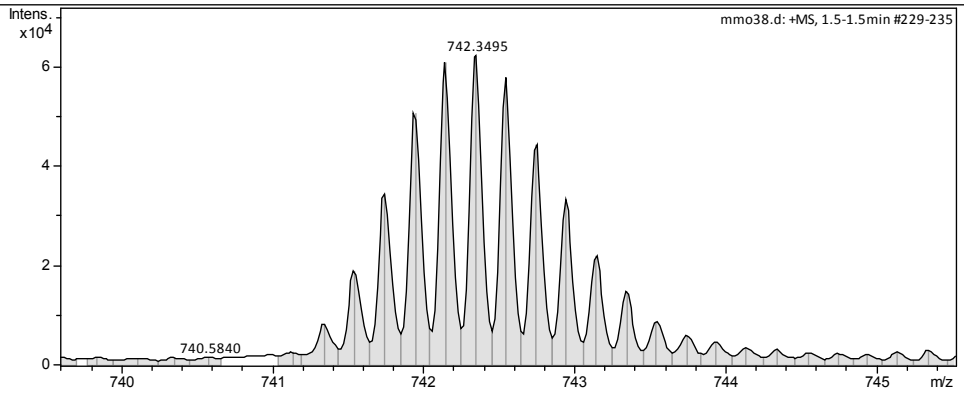
$[M - 6Cl^-]^{6+}$ Calc. 612.6295	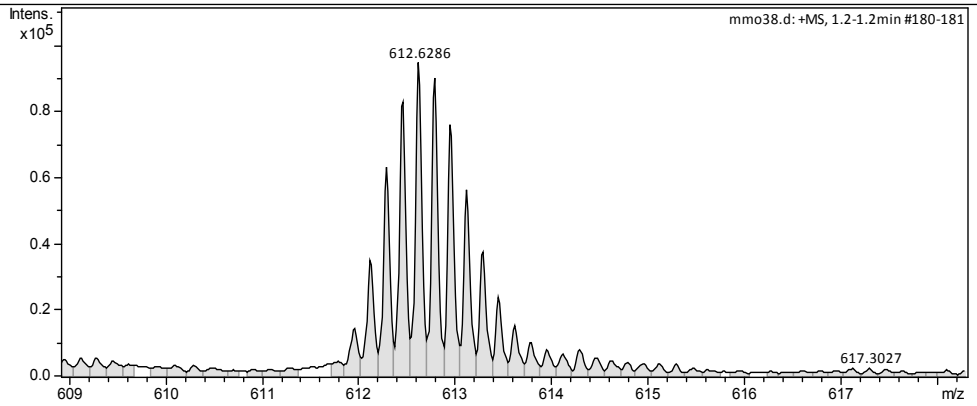
$[M - 7Cl^-]^{7+}$ Calc. 520.1155	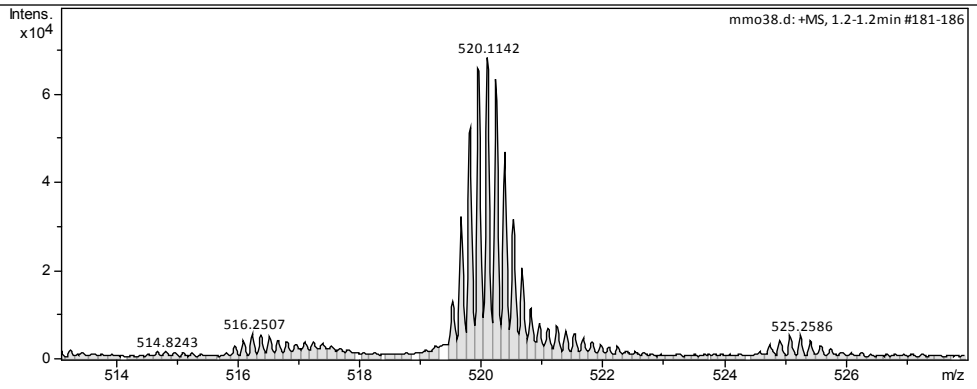
$[M - 7Cl^-]^{7+}$ Calc.450.6049	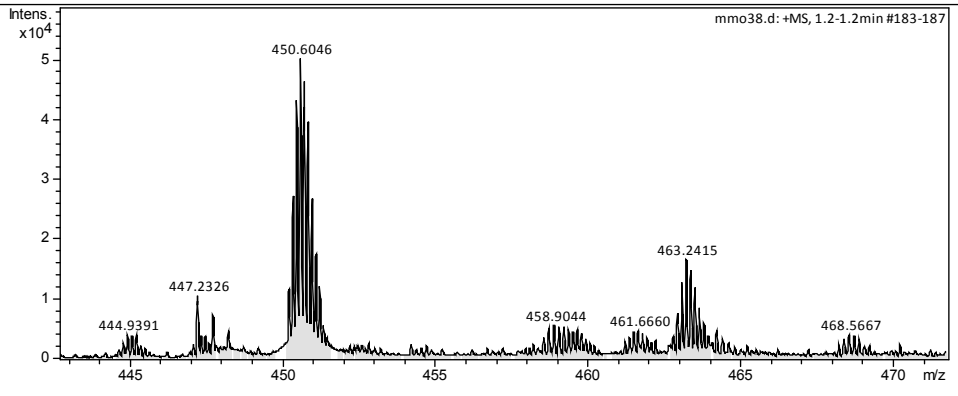

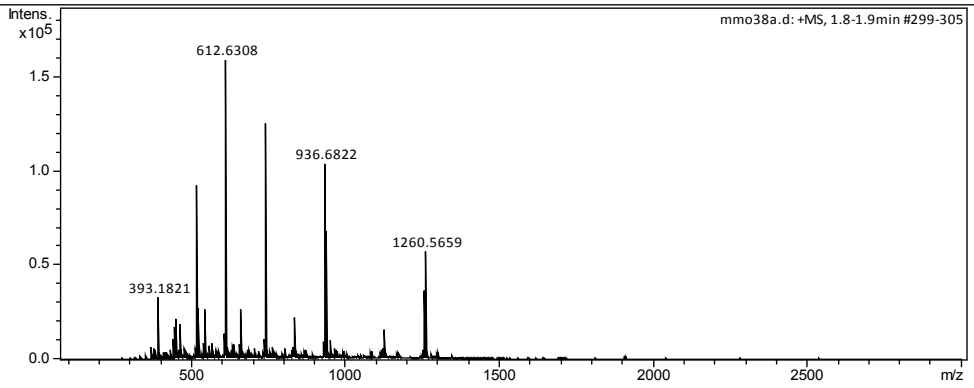
Intens.
x10^5
mmo38a.d: +MS, 1.8-1.9min #299-305
612.6308
936.6822
1260.5659
393.1821
1.5
1.0
0.5
0.0
500
1000
1500
2000
2500
m/z

Table SI3. Solubility of prepared compounds in water.

gen.	PR_3	anion	< 5mg/ml	50 - 100 mg/ml	> 100 mg/ml
1	PMe_3	I^-			
2	PMe_3	I^-			
3	PMe_3	I^-			
1	NMe_3	I^-			
2	NMe_3	I^-			
3	NMe_3	I^-			
1	$P(Et_2)_2(CH_2)_3OH$	I^-			
2	$P(Et_2)_2(CH_2)_3OH$	I^-			
3	$P(Et_2)_2(CH_2)_3OH$	I^-			
1	PBu_3	I^-			
2	PBu_3	I^-			
3	PBu_3	I^-			
1	PBu_3	Cl^-			
2	PBu_3	Cl^-			
3	PBu_3	Cl^-			
1	$P(C_6H_4\text{-}OMe)_3$	I^-			
2	$P(C_6H_4\text{-}OMe)_3$	I^-			
3	$P(C_6H_4\text{-}OMe)_3$	I^-			
1	$P(C_6H_4\text{-}OMe)_3$	Cl^-			
2	$P(C_6H_4\text{-}OMe)_3$	Cl^-			
3	$P(C_6H_4\text{-}OMe)_3$	Cl^-			

Table SI4. Electrostatic potential on the molecular surface (G3)

	NMe_3	PMe_3	$P(Et_2)_2(CH_2)_3OH$	PBu_3	$P(PhOMe)_3$	$P(Ph)_3$
aver [V]	0.137	0.148	0.148	0.138	0.135	0.133
std [V]	0.061	0.067	0.082	0.063	0.097	0.094
min [V]	-0.028	-0.005	-0.348	-0.001	-0.122	-0.098
max [V]	0.397	0.471	0.629	0.691	0.677	0.676

Average (aver), standard deviation (std), minimum (min), maximum (max) values of surface electrostatic potential. Influence of water and Na+, Cl- is taken implicitly in account (APBS calculation).

Figure SI70. Evaluation of G2 dendrimers cytotoxicity based on IC_{50} values.

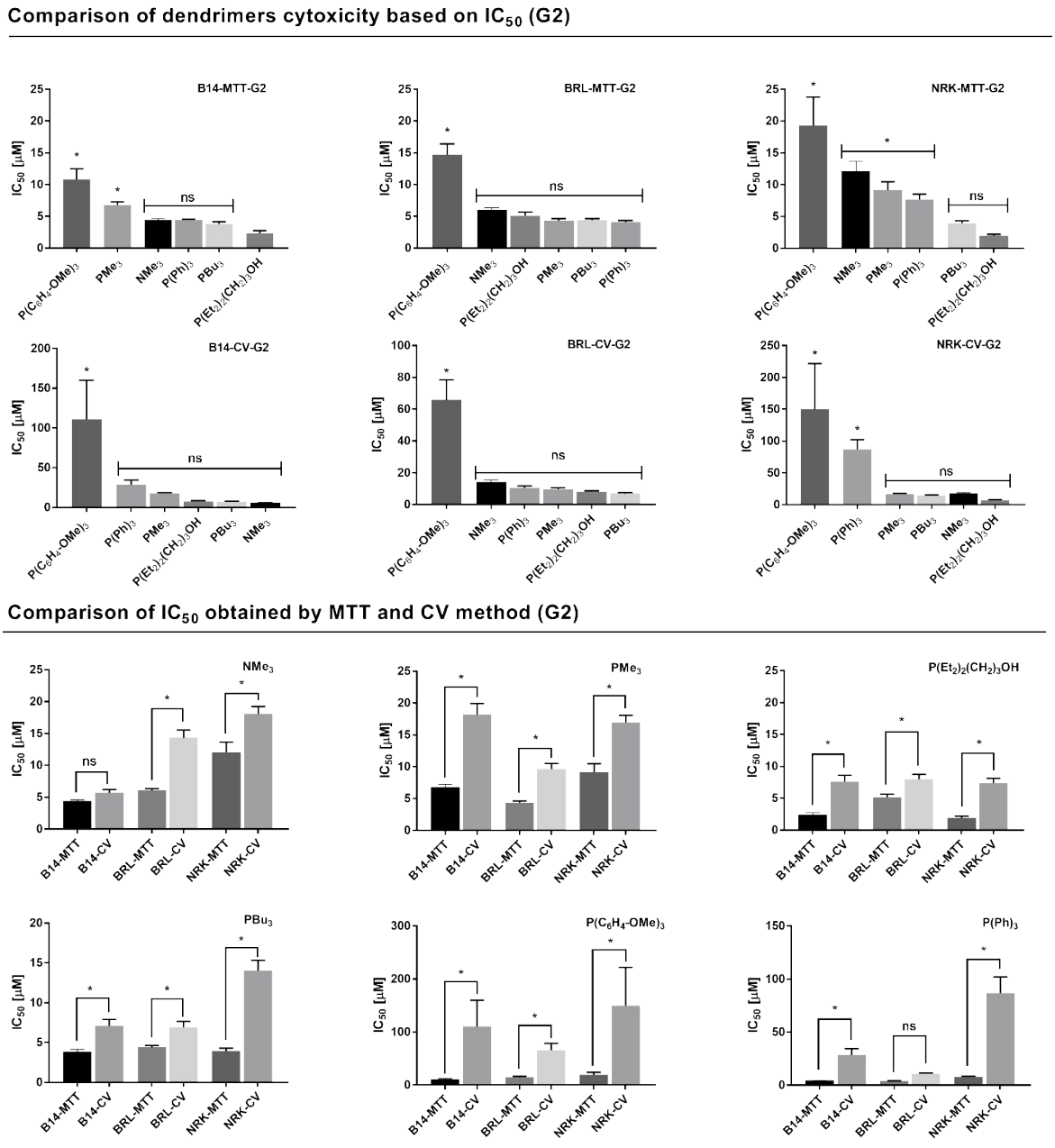

Upper panel: To evaluate and rank cytotoxic effect of each kind of dendrimer based on comparison of IC_{50} values summarized in **Tab. 2**, data of IC_{50} of all dendrimer kinds were plotted in a common column graph for each cell line (B14, BRL, NRK) and assay method used (MTT, CV). Each dendrimer (column) is placed in the order of decreasing mean value of IC_{50} (from left to right, increasing toxicity). In order to determine a statistical significance of difference between the IC_{50} values of all dendrimers, one-way ANOVA followed with Tukey-Kramer multiply comparison test was used to quantify the p values between each dendrimer. Values $p < 0.05$ were supposed to be statistically significant (*), values $p \geq 0.05$ non-significant (ns). Columns were grouped in the graph based on their

p values as compared to lowest IC_{50} mean value present and p values related to their nearest neighbor. Statistical difference between the grouped dendrimers is therefore $p \geq 0.05$ (ns), whereas between groups is $p < 0.05$ (*). In such a manner, a relative order of dendrimer toxicity was constructed for each cell line and assay method used. Data are presented as mean ± SEM (n = 3). *Lower panel:* In order to compare the difference between the toxicity of G2 dendrimers measured by MTT and CV methods, a set of graphs representing IC_{50} values of the same dendrimer assayed by both methods on different cell lines were constructed. In order to determine a statistical significance of difference between the IC_{50} values measured by MTT and CV method for one cell line, unpaired t-test was used to quantify the p values. Values $p < 0.05$ were supposed to be statistically significant (*), values $p \geq 0.05$ non-significant (ns). Data are presented as mean ± SEM (n = 3).

Figure SI71. Evaluation of G1 dendrimers cytotoxicity based on IC_{50} values.

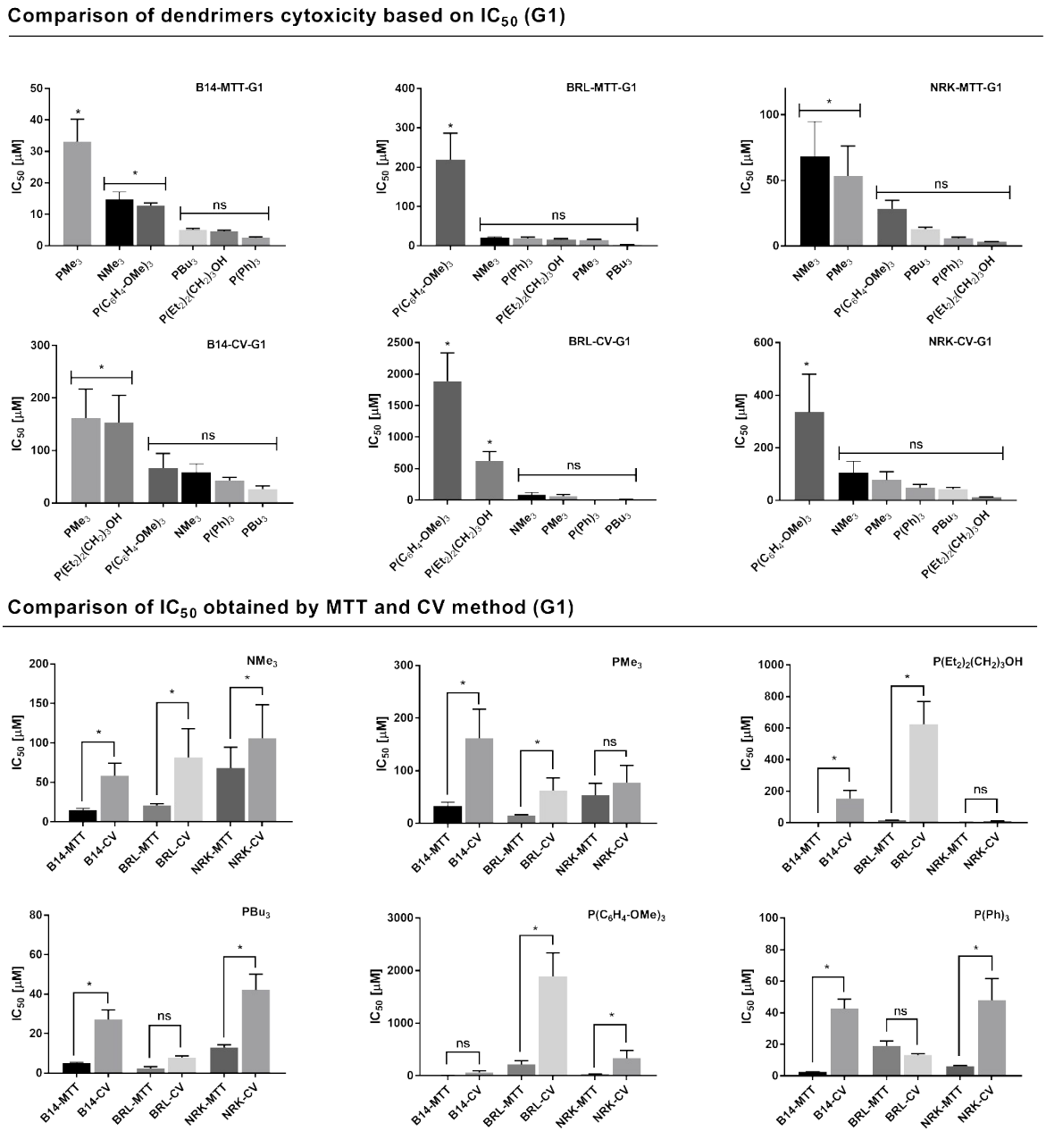

Upper panel: To evaluate and rank cytotoxic effect of each kind of dendrimer based on comparison of IC_{50} values summarized in **Tab.2**, data of IC_{50} of all dendrimer kinds were plotted in a common column graph for each cell line (B14, BRL, NRK) and assay method used (MTT, CV). Each dendrimer (column) is placed in the order of decreasing mean value of IC_{50} (from left to right, increasing toxicity). In order to determine a statistical significance of difference between the IC_{50} values of all dendrimers, one-way ANOVA followed with Tukey-Kramer multiply comparison test was used to quantify the p values between each dendrimer. Values $p < 0.05$ were supposed to be statistically significant (*), values $p \geq 0.05$ non-significant (ns). Columns were grouped in the graph based on their

p values as compared to lowest IC_{50} mean value present and p values related to their nearest neighbor. Statistical difference between the grouped dendrimers is therefore $p \geq 0.05$ (ns), whereas between groups is $p < 0.05$ (*). In such a manner, a relative order of dendrimer toxicity was constructed for each cell line and assay method used. Data are presented as mean ± SEM (n = 3). *Lower panel:* In order to compare the difference between the toxicity of G1 dendrimers measured by MTT and CV methods, a set of graphs representing IC_{50} values of the same dendrimer assayed by both methods on different cell lines were constructed. In order to determine a statistical significance of difference between the IC_{50} values measured by MTT and CV method for one cell line, unpaired t-test was used to quantify the p values. Values $p < 0.05$ were supposed to be statistically significant (*), values $p \geq 0.05$ non-significant (ns). Data are presented as mean ± SEM (n = 3).